MODELING AND MULTIOBJECTIVE OPTIMIZATION OF AN INDUSTRIAL WIPED FILM PET REACTOR USING NSGA – I AND NSGA – II

A Thesis Submitted
In Partial Fulfillment of the Requirements
For the Degree of
MASTER OF TECHNOLOGY

By

Tejas J. Patel

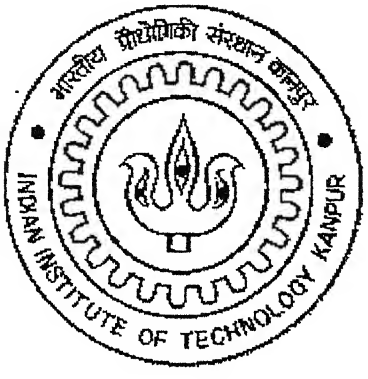

to the

Department of Chemical Engineering
INDIAN INSTITUTE OF TECHNOLOGY, KANPUR

January 2002

CERTIFICATE

This is to certify that the work contained in the thesis entitled 'MODELING AND MULTIOBJECTIVE OPTIMIZATION OF AN INDUSTRIAL WIPED FILM PET REACTOR USING NSGA – I AND NSGA – II ', has been carried out by Mr. Tejas J. Patel, under my supervision and has not been submitted elsewhere for a degree.

Dr. Santosh K. Gupta

Department of Chemical Engineering,
Indian Institute of Technology,
Kanpur – 208016,
India.

ACKNOWLEDGEMENTS

I am very fortunate to be a student of Professor Santosh K. Gupta. I would like to express my gratitude and sincere regards to Professor Gupta for their guidance and constant encouragement throughout the course of this work. I would like to give due acknowledgement to the Department of Chemical Engineering, IIT, Kanpur for having given me an opportunity to work with them.

I am indebted to my parents and members of my family bringing me up to this level.

I would like to thank all my lab mates Rahul, Swarnendu, Anjana, Sameer and Arpan who were always cooperative with me. I would also like to thank all my batch mates Prabhakar, Jeetain, Anurag, Amit, Arun and Rohit, who have been a constant source of encouragement during my stay.

I would also like to thank Professor Ashok Khanna, Professor Y. V. C. Rao, and Professor D.N. Saraf for their support.

My sincere thanks to V. Bhaskar, whose work on Modeling and Optimization of an Industrial Wiped-film PET reactor has been followed in this thesis.

TABLE OF CONTENTS

SUMMARY

An improved two-phase model has been developed for a wiped-film (third stage) PET reactor. The model accounts for all the important main and side reactions and incorporates the effect of vaporization of four low molecular weight volatile species. Industrial data under three different operating conditions are used to obtain best-fit (tuned) values of ten model parameters.

Multiple objectives (often conflicting) occur naturally in polymerization reactors and offer a great deal of challenge and insight when vector optimization is applied to these systems. Polyethylene terephthalate (PET) is one of the most widely used polymers in day-to-day life. The profit margins in synthetic fiber industries (especially PET fibers) are declining and therefore any economic improvement through process optimization would cause a major reduction in the operating costs. In an attempt to achieve this objective, we have undertaken a task of fundamental modeling and multiobjective optimization of the wiped-film finishing reactor as a preliminary step in the process of system optimization. Multiobjective optimization of the third-stage wiped film polyester reactor is then carried out using the 'tuned' model. The two objective functions minimized are the acid and vinyl end group concentrations in the product. These are two of the undesirable side products produced in the reactor. The optimization problem incorporates an end-point constraint to produce polymer having a desired value of the degree of polymerization (DP). In addition, the concentration of the di-ethylene glycol end group in the product is constrained to lie within a certain range. Two adaptations of the nondominated sorting genetic algorithm (NSGA – I and NSGA – II) have been used to solve the above multiobjective optimization problem. The decision variables used are

the reactor pressure, temperature, catalyst concentration, residence time of the polymer inside the reactor and the speed of the agitator. A unique optimal solution was obtained in all cases unlike what was observed in an earlier study [Bhaskar et al. (2000)]. Use of suitable GA parameters is necessary to avoid the problems of sensitivity and premature convergence. A unique optimal solution is obtained even when the objective functions are taken one at a time.

NOMENCLATURE

a	Specific interfacial area per unit volume of the melt, m^{-1}
a_o	Coefficient in the polynomial relating χ_1 to polymer concentration
A	Acetaldehyde
A_l	Cross-sectional area of the melt in the reactor, m^2
b_o	Coefficient in the polynomial relating χ_1 to polymer concentration
DEG	Di-ethylene glycol
DP	Degree of polymerization, or the number average chain length of the polymer
E_a	Acid end groups
E_{DEG}	DEG end groups (excluding those on pure DEG)
E_g	Hydroxyl end groups (excluding those on pure EG)
EG	Ethylene glycol
E_v	Vinyl end groups
f, out	Final, outlet value
$\boldsymbol{I}$	vector of objective functions, I_i
k_1 to k_9	Forward reaction rate constants for Eqs. 1-9 in Table 2.1
k_1', k_5', k_7', k_8'	Reverse reaction rate constants for Eqs. 1,5,7 and 8 in Table 2.1
k_{2o} , k_{3o}, k_{9o}	Frequency factors of reactions 2,3 and 9 (Table 2.1), respectively
k_l	Overall liquid phase mass transfer coefficient, m/min
K_1, K_5, K_7, K_8	Equilibrium constants for Eqs. 1, 5, 7 and 8 in Table 2.1
l_{chrom}	Chromosome length
L	Length of the reactor, m

M_j	Molecular weight of the volatile species, j
m_j	Ratio of liquid-phase molar volume of the polymer and pure species, j
N	Speed of the agitator, RPM
N*	Dimensionless value of N ($\equiv N/N_{ref}$)
N_g	Number of generations in NSGA – I and NSGA - II
N_{gen}	Maximum number of generations in NSGA- I and NSGA - II
N_p	Number of chromosomes in the population, in NSGA – I and NSGA - II
p_c	Crossover probability in NSGA – I and NSGA - II
p_m	Mutation probability in NSGA – I and NSGA - II
P	Pressure of the reactor, mm Hg or kPa
P_e	Penalty value
Q	Volumetric flow rate of liquid in the reactor, m^3/min
R	Universal gas constant = 8.314 J/(mol-K)
R_1 to R_9	Reaction rate terms
Sh	Sharing function (Eq. 3.2)
S_r	Seed for the random number generator in NSGA– I and NSGA – II
t	Time, min
T	Temperature, K
$\boldsymbol{u}$	Vector of decision variables, u_I
U_V	Volume fraction of volatile material in the melt
U_V°	Volume fraction of volatile material in the melt at z = 0

V_p	Molar volume of pure liquid polymer, kmol/m^3
w_1, w_2, w_3	Weighting factors used in the objective functions
W	Water
$\boldsymbol{x}$	Vector of state variables, x_I
x_j^*	Melt phase mole fraction of the volatile species, j, at the interface (at equilibrium)
x_m	Monomer conversion
y_j	Equilibrium mole fraction of the volatile species, j, in the vapor space
z	Dimensionless axial location in reactor (≡ axial position/L)
Z	Di-ester groups

Greek Alphabets

α	Exponent describing the effect of agitator speed on k_la
α_{sh}	Exponent controlling the sharing effect in NSGA – I
γ_j	Activity coefficient of the volatile species, j
θ	Residence time, min ($\equiv A_lL/Q$)
θ^*	Dimensionless value of θ ($\equiv \theta/\theta_{ref}$)
μ_n	Number average chain length of polymer
ρ_j	Density of the pure liquid species, j, kg/m^3
σ	Maximum normalized distance in $\boldsymbol{u}$ space between any two points in NSGA - I
χ_1	Flory parameter describing vapor-liquid equilibrium

Symbols

[•]	Concentration in the melt, $kmol/m^3$ (unless otherwise specified)

Subscripts / Superscripts

d	Desired value
f	Feed value
out	Outlet value
0	Value at z = 0 (inlet of reactor)
ref	Reference conditions, as in Bhaskar et al. (2000)

LIST OF TABLES

Chapter 2

Chapter 4

LIST OF FIGURES

Chapter 3

Chapter 4

Chapter 1: INTRODUCTION

Present day chemical engineering is associated with core competencies in four major areas: reaction engineering, transport phenomena, separations science, and computational and systems science. Several paradigm shifts have taken place in this discipline over the years. These include the introduction of mathematical modeling in its various forms (including process control, systems approach, etc.), the shift from unit operations to transport phenomena, the recent transition towards biosystems, etc. However, one facet of chemical engineers remains unchanged, namely that they have a responsibility of integrating the chemical engineering core constituencies with economic parameters so as to achieve commercial success. In this context, optimization of chemical processes plays a key role in chemical engineering. Optimization techniques have been applied to problems of industrial importance ever since the late 1940s, and several excellent texts (Beveridge and Schechter, 1970; Bryson and Ho, 1969; Edgar and Himmelblau, 1988; Lapidus and Luus, 1967; Ray and Szekely, 1973) describe the various methods with examples. The complexity of the problems studied has increased as faster and more powerful computational hardware and software have become available. The solutions of even more sophisticated optimization problems will become available as complex biosystems are studied and get exploited commercially in the future. In this decade, particularly, several industrial systems have been optimized, which involve multiple objective functions and constraints, using a variety of mathematical techniques and robust computational algorithms. In a few cases, the optimal solutions have been implemented in industry with some success.

Optimization of chemical processes has been a fascinating field of study for several decades. Until about 1980, virtually all problems in chemical engineering were optimized using *single* objective functions. Often, the objective function (also called the cost function) accounted

for the economic efficiency only, which is a scalar quantity. The reason for solving such relatively simple optimization problems was possibly, the limitations posed by the technology of computing systems. Most real world chemical engineering problems require the simultaneous optimization of *several* objectives (multiobjective optimization), which cannot be compared easily with each other (are non-commensurate), and so cannot be combined into a single, meaningful scalar objective function. Examples include reliability, safety, hazard analysis, control performance, environmental quality, etc., apart from the major goal of achieving economic efficiency. Until a few years ago, these several objective functions were combined into a single scalar objective function, using arbitrary weight factors, so that the problem could become computationally tractable. This 'scalarization' of what is really a vector objective function suffers from several drawbacks. One is that the results are sensitive to the values of the weighting factors used, which are difficult to assign on an *a-priori* basis. What is even more important is the less-recognized fact that there is a risk of losing some optimal solutions (Chankong and Haimes, 1983; Haimes, 1977). Therefore, it may be necessary that a *vector* form of all the objective functions be used in formulating and solving real-life optimization problems.

The concept of multiobjective optimization is attributed to the economist, Pareto (1896). After several decades, this concept was recognized in operations research and has recently become popular in engineering. There have been several applications of multiobjective optimization in chemical engineering. Polymerization reactor optimal design and control problems are inevitably multiobjective in nature. Unique problems in polymerization reactors are encountered in the area of optimal design and control. This is because of the fact that the quality of the polymer is defined in abstract terms such as strength, processability, stiffness, crimp, etc. Though these terms can be correlated to more quantifiable properties like molecular weight

distribution and the composition, the definition of meaningful optimization problems always ends up in the formulation of a multiobjective optimization problem.

The aim of this study is to apply multiobjective optimization on the industrial polyethylene terephthalate reactor. Polyethylene terephthalate (PET), commonly referred to as polyester, is one of the most commonly used polymers with diverse applications like synthetic fibres, films, bottles, engineering applications, etc. Commercially, PET is manufactured in three stages using continuous reactors. The first stage (esterification stage) is carried out at atmospheric pressure and at 270-280°C. The raw materials commonly used are a molar excess of ethylene glycol (EG) and either purified terephthalic acid (PTA) or dimethyl terephthalate (DMT). PTA and DMT have their own advantages and disadvantages. Nowadays, DMT is not usually preferred because of the problems in handling methanol, a by-product in the first stage. The use of PTA posed a problem earlier because its solubility in EG is low. But it has good solubility in BHET (bis-hydroxy ethylene terephthalate), a product of the first stage reactor, and the use of a recycle stream (or back mixing) in the first stage can overcome this drawback. PTA and EG are now usually processed in a series of CSTRs or a plug flow reactor with a recycle in the first (or esterification) stage. A polycondensation catalyst, antimony trioxide, is injected in small concentrations (0.03 – 0.05 percent by weight) into the oligomer stream exiting from this reactor. The second stage (pre-polymerization) is carried out either in one or two agitated vessels under reduced pressures, at about 15-30 mm Hg and 270-280^{0}C. The degree of polymerization, DP, reaches a value of about 30-40 in this stage. The prepolymer so produced undergoes final polycondensation in a finishing (or third stage) reactor in which the pressure is maintained quite low at 1-2 mm Hg, at a temperature of about 280-290^{0}C. Since the reaction mass is very viscous under these conditions, the finishing reactor has a special construction to enhance mass transfer

and the removal of the by-product, ethylene glycol, so as to drive the reaction in the forward direction and to give a product having a high value of DP. The finisher is usually a jacketed cylindrical vessel with a horizontal agitator, with large screens mounted on the latter. The reaction mass in the third-stage reactor is usually heated by condensing Dowtherm™ vapors in a jacket. The desired DP of the product (textile grade) from this reactor is above about 80. In the finishing reactor, a complex series of reactions accompanies the main polycondensation reaction. Apart from playing an important role in controlling the product quality (such as fiber color, dyeability and stability), these side reactions also modify the progress of polymerization. There is an absolute need for meeting the stringent industrial product specifications through more effective operation these days. For example, a small change in di-ethylene glycol end group concentration, $[E_{DEG}]$, in the polymer affects polymer crystallinity, melting point and dyeability of the polyester. Such polymer properties are very difficult or impossible to measure on–line. Thus, it is very difficult to control the polymer product quality due to delayed off-line laboratory measurements. Therefore, any insight into the optimal operation of the finishing stage leading to improved productivity and product quality control is extremely useful.

Having understood the need for optimization of finishing reactors, one must decide on suitable methodologies to solve the problem. Numerous optimization techniques are available for solving multiobjective optimization problems (Chankong and Haimes, 1983; Srinivas and Deb, 1995). These days, with the advent of high speed computing machines and the availability of powerful computational software, there has been a shift towards evolutionary techniques that yield comparatively much better results for complex problems with multiple solutions. One such technique that has rapidly gained acceptance in the recent past is Genetic Algorithm (GA). GA is

noted for its robustness and ability to find the global optimum where most other methods end up in local optima. The reasons favoring the use of GA are:

- Objective functions can be multimodal or discontinuous.
- Only information on the value of the objective function is required; gradient evaluation is not required.
- A starting point is not needed, and the search is from a randomly generated population of points.
- It is better suited to handle large problems involving many variables.

Moreover, GA can be adapted to effectively handle real-life problems involving the optimization of two or more objective functions simultaneously, as applied in this study. Non-dominated sorting genetic algorithm (NSGA - I), a popular adaptation of GA (Srinivas and Deb, 1995), has been very efficient in solving multiobjective optimization problems. Indeed several problems in chemical engineering have been solved using NSGA - I (Garg and Gupta, 1999; Mitra et al., 1998).

The model developed and tuned on some industrial data [Bhaskar et al. (2000a)] was re–tuned in this study since some minor errors were found in the previous study. This is described in Chapter 2. Chapter 3 describes NSGA – I as well as a more recent adaptation referred to as the *elitist* Non–dominated Sorting Genetic Algorithm, NSGA – II [Deb and coworkers (2000)]. Chapter 4 compares the results of the multiobjective optimization problem using both NSGA – I and NSGA - II. Finally, appropriate conclusions are made on the study and suggestions for future work are indicated in Chapter 5.

Chapter 2: MODELING AND SIMULATION

2.1 Introduction

Poly (ethylene terephthalate) (PET) is one of the most widely used polymers in the fiber and engineering plastics industry. In the past two decades, PET has gained sufficient commercial importance to inspire a considerable amount of research in the area of modeling and simulation of the several reactors used in its manufacture. The early 1980s saw work in the open literature in this area primarily from two groups in India, ours (Kumar et al., 1982 a, b; 1983) and that of Ravindranath and Mashelkar (1982 a, b). After a short period of reduced interest, this area again started attracting considerable interest from groups led by Choi (Besnoin and Choi, 1989; Lei and Choi, 1990; Laubriet et al., 1991; Cheong and Choi, 1995, 1996), Ray (Hipp and Ray, 1996; Jacobsen and Ray, 1992a) and Doherty and Malone (Steppan et al., 1990). Several reviews have also appeared over these last two decades in this area (Gupta, 1983; Ravindranath and Mashelkar, 1986 a, b; Jacobsen and Ray, 1992b). The finishing reactor for PET poses interesting problems in modeling due to the coupling of the mass-transfer and kinetic effects. In the past few years, several attempts have been made to develop models for this reactor. These vary in their levels of sophistication, from the earliest and simplest models (Secor, 1969; Hovenkamp, 1971; Amon and Denson, 1980; Ravindranath and Mashelkar, 1982c, 1984; Ghosh et al., 1983; Gupta et al., 1984; Kumar et al., 1984a) to more recent ones (Laubriet et al., 1991; Cheong and Choi, 1995, 1996; Jacobsen and Ray, 1992a; Hipp and Ray, 1996) incorporating not only the main reactions but also several side reactions taking place in the reactors. Secor (1969) was the first to use penetration theory to explain mass transfer effects in a finishing reactor. The calculations use a value of 1.0 for the equilibrium constant for the polycondensation reaction. Hovenkamp (1971) made use of the Flory–Huggins (Flory, 1953) model instead of Raoult's law, to predict the

activity coefficients of the different vaporizing species, EG, as well as other low molecular weight compounds produced by the side reactions, namely, water (W) and diethylene glycol (DEG). Amon and Denson (1980) proposed a simplified analysis for the performance of wiped film reactors. Gupta et al. (1983) and Kumar et al. (1984a) made modifications in this model and extended it for predicting the poly-dispersity index of the polymer using moment-closure techniques (Gupta and Kumar, 1987). Ravindranath and Mashelkar (1982a) developed an effective flash procedure for determining the interfacial concentration of the volatile species along the length of the finisher. Disc-ring reactor models and axial dispersion plug flow models were proposed by Dietze and Kunhe (1969) and Ravindranath and Mashelkar (1982c) for describing the performance of these reactors. Laubriet et al. (1991) proposed a two-phase model for the finishing reactor for the polycondensation of PET. This model has the advantage of being independent of the specific reactor geometry, since it uses a *single* variable, k_La, to describe the mass transfer effects in the reactor. Cheong and Choi (1995, 1996) proposed a multi-compartment model for the continuous rotating disc polycondensation reactors. This model does not consider the side reactions that occur in the reactor. A detailed kinetic modeling study has been done by Jacobsen and Ray (1992a) who solve the equations using their CAD package, POLYRED. Hipp and Ray (1996) have developed a dynamic model for polycondensation in tubular reactors.

Bhaskar et al.(2000a) used the two phase model of Laubriet et al.(1991) and tuned the model–parameters so as to describe a third stage wiped film *industrial* PET reactor. A few errors were detected in the computer code used. In this study, we re–tuned ten parameters of Bhaskar et al. (2000a) using genetic algorithm (GA). This re–tuned model is then used to obtain optimal operating conditions for this reactor, using multiple objective functions and end point

constraints. The technique used in this study is quite general, and parallels similar work on the modeling of an industrial nylon-6 semibatch reactor (Wajge et al., 1994).

2.2 Formulation

The kinetic scheme used in the present work is presented in Table 2.1. Apart from the main polycondensation reaction, the side reactions considered are the formation of acetaldehyde (A), DEG, water (W) and the degradation of di-ester groups (Z). The reactions taking place in the finishing reactor are quite complex. Unfortunately, kinetic information is not available for many of the side reactions, and even for the main reactions is, at best, unreliable. The choice of the side reactions is based on the objectives of modeling and on the level of sophistication we wish to have in predicting the product properties. We have considered all the main reactions (Equations 1-9, Table 2.1). These have *also* been used for modeling by Bhaskar et al.(2000a). The concentrations of several of the other by-products are extremely low under conditions of interest and therefore, in all engineering applications and for *computational ease,* one has usually ignored them. For example, cyclic oligomers have been ignored by Ravindranath and Mashelkar, (1986a) and Laubriet et al. (1991).

The steady-state model equations are quite similar to those presented by Laubriet et al. (1991) and the complete set is summarized in Table 2.2. It is assumed that the flow of the liquid down the reactor is plug-flow and that the vapor phase is well mixed. Also, it is assumed that there is no mass transfer resistance in the vapor phase. Flory-Huggins' theory (Flory, 1953) is used to describe the activity coefficients of three of the four volatile species, EG, W and DEG. The other species, acetaldehyde, is assumed to vaporize as soon as it is produced in the liquid phase. Most of the details of the model development are available in the literature [Bhaskar et al. (2000a)] and are not repeated here. Bhaskar et al. (2000a) tuned nine parameters in the model.

TABLE 2.1: Kinetic scheme and kinetic parameters

1. Ester interchange reaction (Main Polycondensation)

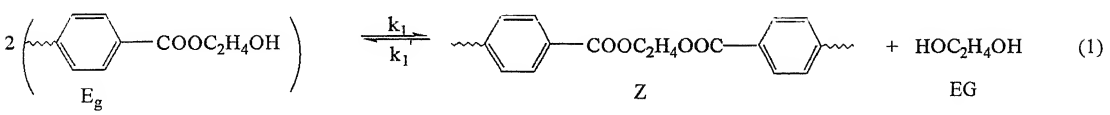

2. Acetaldehyde Formation

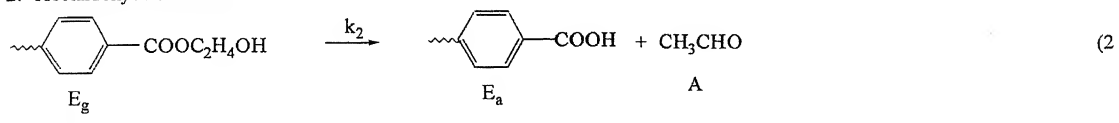

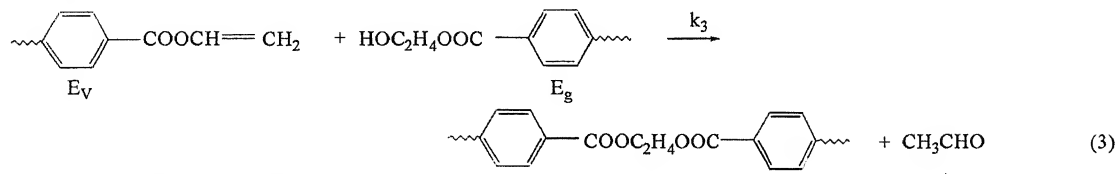

3. Diethylene Glycol Formation

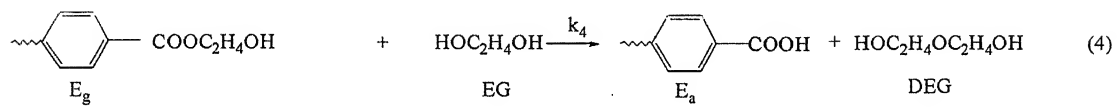

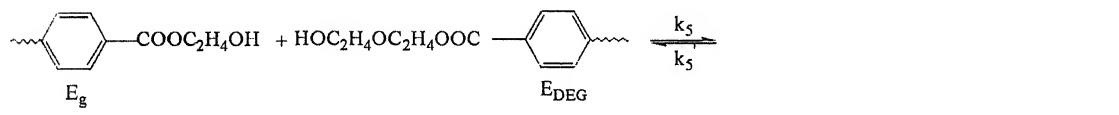

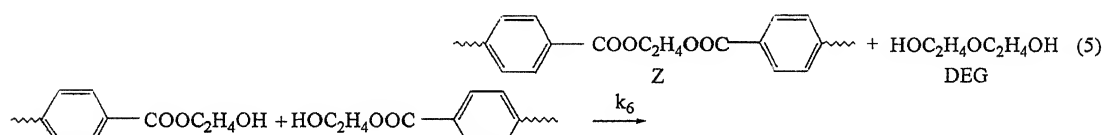

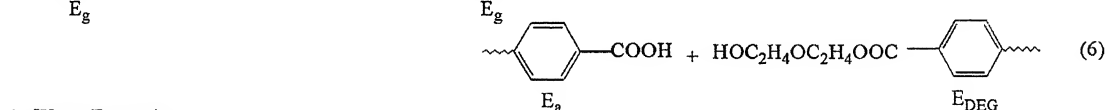

4. Water Formation

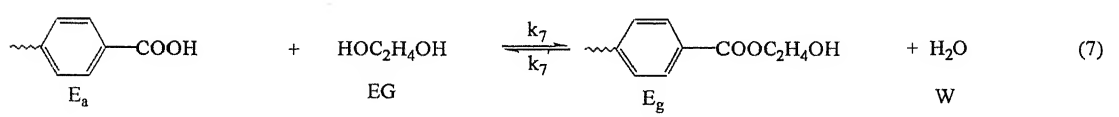

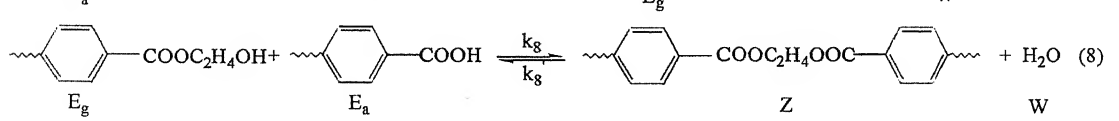

5. Degradation of Diester group

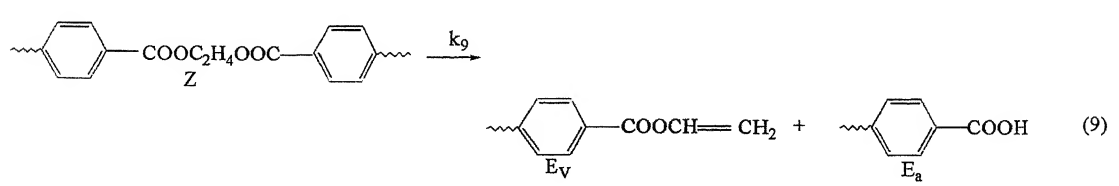

Table 2.1 Continued.....

Kinetic parameters (Bhaskar et al. (2000))([Sb_2O_3] = 0.04 wt %)$^+$

Reaction No., i	**Type of reaction**	**Rate constant** $k_i = k_{io} \exp(-E_i/RT)$		**Equilibrium constant**
		k_{io} (m^3 mol^{-1} min^{-1})	**E_i (J mol^{-1})**	
1	Reversible	1.09×10^3	77441	5.1400
2	Irreversible	2.7480×10^7*	124742	
3	Irreversible	2.245×10^3	77441	
4	Irreversible	8.32×10^4	124742	
5	Reversible	1.09×10^3	77441	2.871×10^{-2}
6	Irreversible	8.32×10^4	124742	
7	Reversible	2.08×10^3	73673	2.5
8	Reversible	2.08×10^3	73673	10.340
9	Irreversible	0.6395×10^9*	158230	

+ Values of K_1, K_5, K_8, k_{2o}, k_{9o} and k_{3o} are those obtained in the present study, and differ from those of Bhaskar et al. (2000a) .

*min^{-1}

TABLE 2.2: Complete set of model equations used in this study

Balance equations for the liquid phase [Laubriet et al. (1991)]

$$\frac{1}{\theta}\frac{d[E_g]}{dz} = [-2R_1 - R_2 - R_3 - R_4 - R_5 - 2R_6 + R_7 - R_8]$$

$$\frac{1}{\theta}\frac{d[E_a]}{dz} = [R_2 + R_4 + R_6 - R_7 - R_8 + R_9]$$

$$\frac{1}{\theta}\frac{d[Z]}{dz} = [R_1 + R_3 + R_5 + R_8 - R_9]$$

$$\frac{1}{\theta}\frac{d[E_v]}{dz} = [-R_3 + R_9]$$

$$\frac{1}{\theta}\frac{d[E_{DEG}]}{dz} = [-R_5 + R_6]$$

$$\frac{1}{\theta}\frac{d[EG]}{dz} = R_1 - R_4 - R_7 - k_l a([EG] - [EG^*])$$

$$\frac{1}{\theta}\frac{d[W]}{dz} = R_7 + R_8 - k_l a([W] - [W^*])$$

$$\frac{1}{\theta}\frac{d[DEG]}{dz} = R_4 + R_5 - k_l a([DEG] - [DEG^*])$$

where :

$R_1 = k_1[E_g]^2 - 4k_1'[Z][EG]$

$R_2 = k_2[E_g]$

$R_3 = k_3[E_v][E_g]$

$R_4 = 2k_4[E_g][EG]$

$R_5 = k_5[E_g][E_{DEG}] - 4k_5'[Z][DEG]$

$R_6 = k_6[E_g]^2$

$R_7 = 2k_7[E_a][EG] - k_7'[E_g][W]$

$R_8 = k_8[E_g][E_a] - 2k_8'[Z][W]$

$R_9 = k_9[Z]$

Vapor-liquid equilibrium correlations:

$$C_j^* = \left(\frac{C_{poly}}{1 - \sum_j x_j^*} \right) x_j^* \quad ; \quad C_j^* = [EG^*],\ [W^*],\ [DEG^*]$$

$$C_{poly} = \frac{[E_g] + [E_a] + [E_v] + [E_{DEG}]}{2}$$

$$x_j^* = \frac{Py_j}{P_j^o \gamma_j} \quad ; \ j = EG,\ W,\ DEG$$

$$\ln P_{EG}^o = 49.703 - (8576.7/T) - 4.042 \ln T$$

$$\ln P_W^o = 18.568 - \frac{4047.606}{T - 33.3}$$

$$\ln P_{DEG}^o = 17.0326 - \frac{4122.52}{T - 122.5}$$

$$y_j = \frac{\int_0^1 k_l a (C_j - C_j^*) dz}{\sum_j \int_0^1 k_l a (C_j - C_j^*) dz + \int_0^1 (k_2 [E_g] + k_3 [E_v][E_g]) dz} \quad j = EG,\ W,\ DEG$$

$$\gamma_j = \frac{1}{m_j} \exp\left(1 - \frac{1}{m_j} + \chi_1 \right) \quad ; \ j = EG,\ W,\ DEG$$

$$m_j = \frac{V_p \rho_j}{M_j} \quad ; \ j = EG,\ W,\ DEG$$

$$U_v = \sum_j \frac{M_j C_j}{\rho_j} \quad ; \ j = EG,\ W,\ DEG$$

$$V_p = \frac{1 - U_v}{C_{poly}}$$

$$\chi_1 = a_o + b_o \left(1 - \frac{U_v}{U_v^o} \right)$$

$$k_l a = k_l a_{ref} \left(\frac{N}{N_{ref}} \right)^{\alpha}$$

$$DP = \left(\frac{([E_g] + [E_a] + [E_v] + [E_{DEG}] + 2[Z])_{feed}}{[E_g] + [E_a] + [E_v] + [E_{DEG}]} \right)$$

We have re–tuned all these nine parameters. Upon re–tuning, however, we found that the value of $[E_v]_{out}$, the concentration of vinyl end groups in the product, does not match the industrial value. As a result, a tenth parameter, k_{30}, was also tuned in the present study. The model equations (Table 2.2) for the reactor are a set of ordinary differential equations (ODEs). These are to be integrated using appropriate values of the feed conditions. These are given in Table 2.3 [Bhaskar et al (2000a)]. The NAG subroutine, D02EJF, was used to solve these equations. The subroutine uses Gear's algorithm (Gupta, 1995) with a tolerance of 10^{-12}. An iterative solution is necessary because the liquid and vapor phases have different kinds of flow (plug and well–mixed). Values for the average mole fractions of the three of the four volatile species in the vapor phase, y_j, are assumed (see Table 2.4 for the starting guess values) and then the ODE's are integrated from the dimensionless value of z = 0 (feed end) to z = 1 (product end). The vapor phase values of y_j are then re-evaluated and used as the guess values for the next iteration. This method of successive substitutions (Picard iteration) (Gupta, 1995) is continued till the sum of the squares of the y_j does not change between two successive iterations by more than 1×10^{-12}. The program was run on a P3 (586 MHz) computer, on a Linux platform. The model provides values of DP and the concentrations of the hydroxyl end groups (E_g), acid end groups (E_a), di-ester end groups (Z), vinyl end groups (E_v), DEG end groups (E_{DEG}), ethylene glycol (EG), water (W) and di-ethylene glycol (DEG), as a function of the axial position in the reactor after convergence is achieved.

Four sets of industrial data were available. These are the same as used by Bhaskar et al. (2000a) and are given in Table 2.5. In order to obtain best-fit (tuned) values of the parameters in the model, an error function, I, is defined. This comprised of a sum of square errors between the model predicted and industrial values:

Table 2.3 Feed conditions [Bhaskar et al. (2000a)]

Feed concentrations, Kmol/m^3	Densities of pure liquid components, (kg/m^3)
$[E_g]_f = 4.0\times10^{-1}$	$\rho_{EG} = 1108$
$[E_a]_f = 2.57\times10^{-3}$	$\rho_W = 1000$
$[Z]_f = 11.2$	$\rho_{DEG} = 1118$
$[E_v]_f = 1.17\times10^{-3}$	
$[E_{DEG}]_f = 0.17$	
$[EG]_f = 6.5\times10^{-3}$	
$[W]_f = 4.6\times10^{-4}$	
$[DEG]_f = 4.0\times10^{-4}$	
$DP_f = 40$ *	

* no unit

Table 2.4 Values of parameters used in this study

Initial guess values used for y_j :	Weighting factors used in eqs. 2.3, 2.4 and 2.6
$y_{EG} = 0.93$	$w_{11} = w_{13} = w_{14} = 1\times10^5$
$y_W = 0.0269$	$w_{21} = w_{31} = w_{41} = 1\times10^3$
$y_{DEG} = 0.0246$	

GA parameters used in this study:

$P_c = 0.9$
$P_m = 0.05$
$Sr = 0.149$
$nparam = 10$
$N_p = 100$
$N_{gen} = 100$
$l_{chrom} = 320$

$$I(\underset{\sim}{\mathbf{u}}) = \sum_{i,j} w_{ij} \left[1 - \frac{S_{ij,m}}{Sij_{,ind}} \right]^2 \qquad (2.1)$$

where S_{ij} is the value of the i^{th} property at the output (or product) end for set no. j, the subscripts, m and ind, represent values predicted by the model (for any set of parameters, **u**) and the industrial values, respectively, and w_{ij} are the weight factors indicating the emphasis to be accorded any error of the i^{th} property of set no. j. Genetic algorithm was used to obtain the values of the model parameters which minimize the error, I. The NAG subroutine D02EJF with a tolerance of 1×10^{-12} was used. Several sets of parameters were tried in this study till a reasonable tuning of the model was accomplished. These are described in the next section.

2.3 Results and Discussion

The corrected computer code was tested for the reference case (see Table 2.5), using the values of the parameters of Bhaskar et al. (2000a). It was found that the model values of the product DP was higher, while for the DEG and the acid end group concentrations at the product end, it was lower. So, we re–tuned the nine parameters ($k_L a_{ref}$, a_0, b_0, K_1, K_5, K_8, k_{2o}, k_{9o} and α) in the model. The objective function used was

$$I = w_{11}\left(1 - \frac{DP_{1,m}}{82.00}\right)^2 + w_{21}\left(1 - \frac{[E_{DEG}]_{1,m}}{0.17}\right)^2 + w_{31}\left(1 - \frac{[E_a]_{1,m}}{1.038\times 10^{-3}}\right)^2 + w_{1,3}\left(1 - \frac{DP_{3,m}}{82.70}\right)^2 + w_{14}\left(1 - \frac{DP_{4,m}}{82.30}\right)^2 \qquad (2.2)$$

The parameters, $k_L a_{ref}$, a_0, b_0, K_1, K_5, K_8, k_{2o}, k_{9o} and α were tuned for sets 1, 3 and 4 by minimizing I. It was found that value of $[E_v]_{out}$, the output concentration of vinyl end group did not match with the industrial value. Several simulations were performed to study the effect of the several rate and equilibrium constants used in this work, individually. The frequency factor (k_{3o})

Table 2.5 : Industrial data and predicted values at the outlet end for the 4 data sets*

Set #	Operating Conditions	Product Property	Industrial Value	Model predicted value
1	Reference (ref)#	DP_{out}	82.00	82.07
		$[E_{DEG}]_{out}$, kmol/m^3	0.17	0.1686
		$[E_a]_{out}$, kmol/m^3	1.038×10^{-3}	1.039×10^{-3}
		$[E_v]_{out}$, kmol/m^3	7.8117×10^{-4}	7.8252×10^{-4}
2	T_{ref} + 1 K	DP_{out}	82.60	82.62
3	P_{ref} – 0.5 mm Hg	DP_{out}	82.70	82.70
4	N_{ref} + 0.1 rpm	DP_{out}	82.30	82.30

* Tuned values of Table 2.1 used to generate model-results.

T_{ref} = 566.15 K; P_{ref} = 2.0 mm Hg; $[Sb_2O_3]_{ref}$ = 0.04 wt. %; θ^* = 1.0; N^* = 1.0; For the other sets, only one of these values is different, as indicated.

of the rate constant, k_3 was found to affect $[E_v]_{out}$ most significantly. Hence, k_{30} was also included as the tenth tuning parameter. The objective function used finally is, thus, given by

$$I = w_{11}\left(1-\frac{DP_{1,m}}{82.00}\right)^2 + w_{21}\left(1-\frac{[E_{DEG}]_{1,m}}{0.17}\right)^2 + w_{31}\left(1-\frac{[E_a]}{1.038\times10^{-3}}\right)^2 + w_{41}\left(1-\frac{[E_V]}{7.8117\times10^{-4}}\right)^2 + w_{13}\left(1-\frac{DP_{3,m}}{82.70}\right)^2 + w_{14}\left(1-\frac{DP_{4,m}}{82.30}\right)^2 \quad (2.3)$$

The parameters to be tuned are $k_L a_{ref}$, a_0, b_0, K_1, K_5, K_8, k_{2o}, k_{9o}, α and k_{30}. Table 2.6 lists the upper and lower bounds as well as the final tuned values (using sets 1, 3 and 4) of these parameters. The values of the six kinetic/equilibrium constants are also included in Table 2.6 along with the other (original, Bhaskar et al. (2000)) values. A similar tuning of rate constants as well as a few other parameters have been reported by Zabisky et al. (1992), for an industrial LDPE reactor. The weight factors were chosen by trial and error, to achieve the best curve-fit. The values of the weight factors used are also given in Table 2.4. The FORTRAN 77 program was run on a P3 (586 MHz) computer.

The parameters so obtained could explain the three sets of industrial results (sets 1, 3 and 4) used for tuning, quite well. These are then used *without change*, to *predict* the effect of a change in temperature (set 2). Very good agreement of the value of DP of the product for this case was obtained (see Table 2.5). The fact that the parameters were obtained using three sets of industrial data, and then the model predicted another set of industrial data well, *without re-tuning of these parameters*, indicates that the model accounts for all the physico-chemical phenomena actually present in the industrial reactor quite well.

Table 2.6 Bounds and final tuned values used in this study

Bounds and final tuned values for the parameters describing the reactor/reactions:

Bounds	Tuned Values	Tuned Values of Bhaskar et al (2000)
$3.4 < k_L a_{ref} < 3.8$	3.7670	2.6875
$0.59 < a_o < 0.79$	0.6189	1.0378
$2.0 < b_o < 2.1$	2.0210	2.1838
$4.9 < K_1 < 5.4$	5.1400	6.1835
$0.027 < K_5 < 0.031$	2.871×10^{-2}	5.143×10^{-2}
$10.0 < K_8 < 15.0$	10.340	11.87
$2.4\times10^{7} < k_{2o} < 2.8\times10^{7}$	2.748×10^{7}	4.7674×10^{7}
$5.0\times10^{8} < k_{9o} < 7.0\times10^{8}$	6.395×10^{8}	0.2215×10^{8}
$2.0 < \alpha < 4.0$	2.627	2.6647
$1.0\times10^{6} < k_{3o} < 4.0\times10^{6}$	2.245×10^{6}	Not Tuned (1.09×10^{6})

A sensitivity analysis is now performed by varying one parameter at a time with other parameters fixed at their reference values. The results are shown in Table 2.7. Such a study gives an intuitive feel of the reactor behavior, information that is useful in studies involving reactor optimization and control. The effect of temperature is considered first. The concentration profiles of the side products and the variation of DP along the axial position, z, of the finishing reactor for three different temperatures (564 K, 566 K and 569 K) are presented in Figs. 2.1-2.8. Fig. 2.1 shows the effect of the reactor temperature on the DP of the polymer. It is observed that as the temperature goes up from 564 to 569 K, the value of the DP of the product increases from 80.95 to 83.71. This is the combined effect of temperature on the rate constants, as well as on the equilibrium interfacial concentration, C_j^* (through P_j°), of the volatile species. It is assumed that χ_1 as well as $k_L a_{ref}$ are not much influenced by such a change in temperature. The DP of the polymer increases primarily because of the faster rate of the main (No. 1) reaction in Table 2.1 at higher temperatures, which leads, simultaneously, to a faster rate of vaporization of EG, the concentration of which is lower in the melt (Fig. 2.2). The degradation reaction (No. 9, Table 2.1) is found to be strongly influenced by temperature. Both the acid end group concentration, $[E_a]$, as well as the vinyl end group concentration, $[E_v]$, increase with an increase in the temperature (see Figs. 2.3 and 2.4). These effects agree well with observations made in industry. The vinyl end groups lead to the formation of anhydrides and network structures, and so need to be kept low. Figs. 2.5-2.7 show that $[E_g]$ and the concentration of [DEG], decrease with increasing temperature, while concentration of [W] increases with increasing temperature. $[E_g]$ decreases because the rate of the main reaction (No. 1) increases. The concentration of [DEG] is lower at higher temperatures because of higher rates of vaporization, as was the case with EG. Lower operating temperatures are preferred in industrial operations to avoid high concentrations

Table 2.7 Sensitivity analysis

	Concentration of various species at the reactor outlet in kmol/m^3							
neter	Value	$[E_g]_{out}$	$10^3[E_a]_{out}$	$10^4[E_v]_{out}$	$[E_{DEG}]_{out}$	$10^5[W]_{out}$	$10^5[DEG]_{out}$	DP_{out}
	564	0.1135	0.9890	7.3987	0.1685	1.0427	1.1974	80.95
	566	0.1095	1.0394	7.8252	0.1686	1.0881	1.1557	82.07
	569	0.1038	1.1278	8.5848	0.1687	1.1678	1.0959	83.71
	0.50	0.1039	1.0230	7.9791	0.1675	0.8457	1.0759	84.06
	1.00	0.1057	1.0282	7.9277	0.1680	0.9236	1.1039	83.37
	1.50	0.1076	1.0336	7.8764	0.1683	1.0044	1.1303	82.70
	2.00	0.1095	1.0394	7.8252	0.1686	1.0881	1.1557	82.07
	0.92	0.1157	1.0373	7.6413	0.1686	1.1338	1.2208	80.27
	0.96	0.1125	1.0379	7.7309	0.1686	1.1098	1.1872	81.19
	1.00	0.1095	1.0394	7.8252	0.1686	1.0881	1.1557	82.07
	1.04	0.1067	1.0417	7.9237	0.1686	1.0685	1.1261	82.91
	3.00	0.1280	0.9851	7.1064	0.1685	1.2088	1.3508	77.04
	3.50	0.1177	1.0127	7.4868	0.1685	1.1411	1.2423	79.76
	4.00	0.1095	1.0394	7.8252	0.1686	1.0881	1.1557	82.07
	4.25	0.1060	1.0523	7.9807	0.1686	1.0650	1.1187	83.09
	0.90	0.1095	1.0395	7.8232	0.1686	1.0895	1.1562	82.05
	1.00	0.1095	1.0394	7.8252	0.1686	1.0881	1.1557	82.07
	1.05	0.1095	1.0394	7.8262	0.1686	1.0873	1.1554	82.08
	1.25	0.1094	1.0392	7.8300	0.1685	1.0845	1.1543	82.11
	1.00	0.1095	1.0394	7.8252	0.1686	1.0881	1.1557	82.07
	1.05	0.1088	1.0373	7.8420	0.1685	1.0575	1.1468	82.29
	1.15	0.1077	1.0336	7.8718	0.1683	1.0050	1.1311	82.67
	1.25	0.1067	1.0307	7.8971	0.1682	0.9622	1.1176	83.01
	3.000	0.1126	1.0749	7.6925	0.1689	1.3226	1.1905	81.08
	3.500	0.1104	1.0500	7.7848	0.1687	1.1570	1.1661	81.77
	3.767	0.1095	1.0394	7.8252	0.1686	1.0881	1.1557	82.07

4.0	0.1144	1.0247	7.6433	0.1686	1.1205	1.2077	80.66
5.0	0.1100	1.0379	7.8067	0.1686	1.0913	1.1609	81.92
6.0	0.1069	1.0475	7.9222	0.1686	1.0712	1.1287	82.82
6.5	0.1057	1.0514	7.9682	0.1686	1.0634	1.1161	83.17
0.15	0.1098	1.0383	7.8117	0.1697	1.0911	0.6129	81.63
0.25	0.1096	1.0391	7.8216	0.1689	1.0889	1.0104	81.95
0.30	0.1095	1.0395	7.8265	0.1685	1.0878	1.2059	82.11
0.35	0.1093	1.0399	7.8313	0.1681	1.0867	1.3993	82.26
9.0	0.1095	1.0717	7.8249	0.1686	1.0865	1.1557	82.06
10.0	0.1095	1.0468	7.8251	0.1686	1.0877	1.1557	82.07
11.0	0.1095	1.0264	7.8253	0.1686	1.0887	1.1557	82.07
12.0	0.1095	1.0093	7.8255	0.1686	1.0895	1.1556	82.08
2.00	0.1097	0.9591	7.8203	0.1686	1.0158	1.1574	82.04
3.00	0.1094	1.0665	7.8269	0.1686	1.1123	1.1551	82.08
4.00	0.1092	1.1737	7.8334	0.1686	1.2084	1.1527	82.11
5.00	0.1090	1.2809	7.8400	0.1686	1.3044	1.1504	82.14
1.0	0.1096	1.0390	13.0170	0.1686	1.0987	1.1574	81.87
2.0	0.1095	1.0394	8.5652	0.1686	1.0883	1.1559	82.04
3.0	0.1094	1.0395	6.0973	0.1686	1.0877	1.1552	82.13
4.0	0.1094	1.0396	4.6564	0.1686	1.0874	1.1550	82.18
5.0	0.1096	0.9486	6.6074	0.1686	1.0088	1.1569	82.10
6.0	0.1095	1.0137	7.4803	0.1686	1.0656	1.1560	82.08
7.0	0.1094	1.0788	8.3535	0.1686	1.1224	1.1552	82.06
8.0	0.1094	1.1440	9.2271	0.1686	1.1791	1.1543	82.03

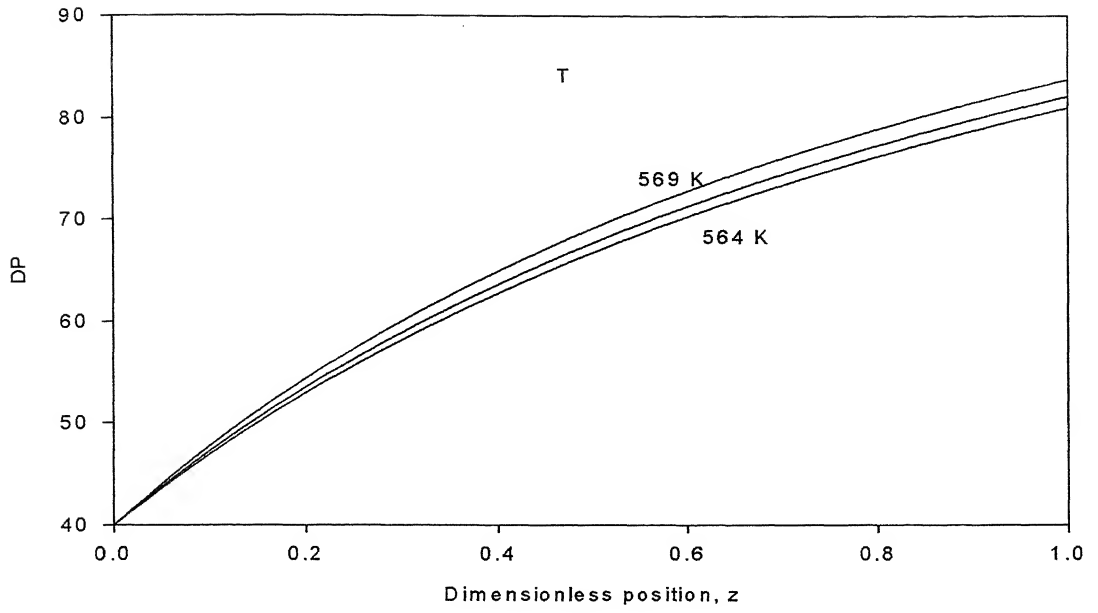

Figure. 2.1 Effect of temperature on the DP of the polymer as a function of the dimensionless axial position in the reactor, z. The unmarked curve represents the variation of DP *vs.* z at the reference temperature of 566 K.

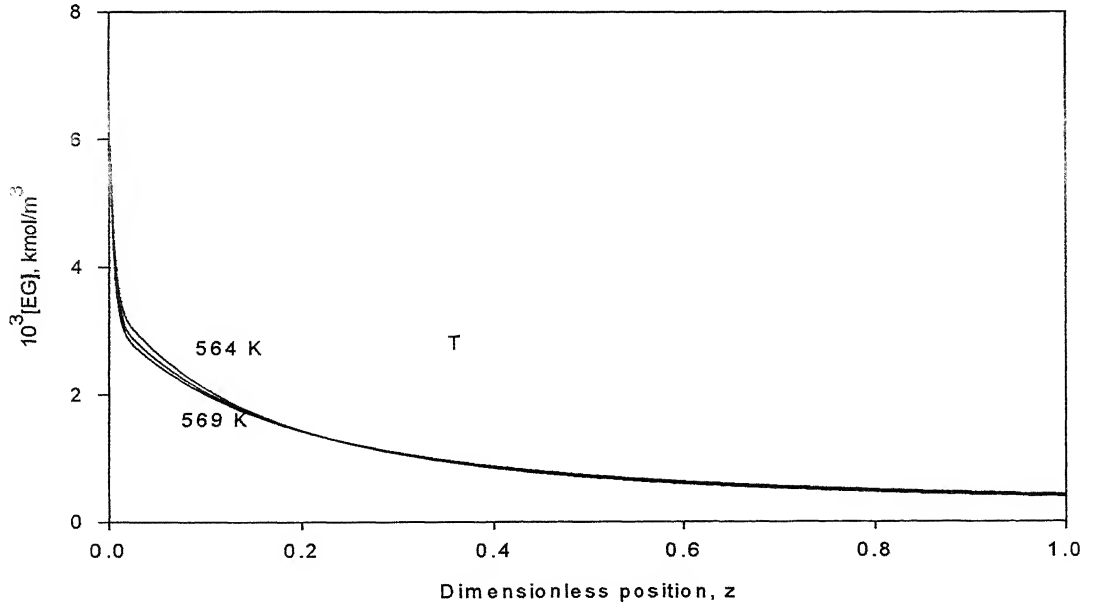

Figure. 2.2 Effect of temperature on the variation of the ethylene glycol concentration, [EG], with z. The unmarked curve corresponds to 566 K.

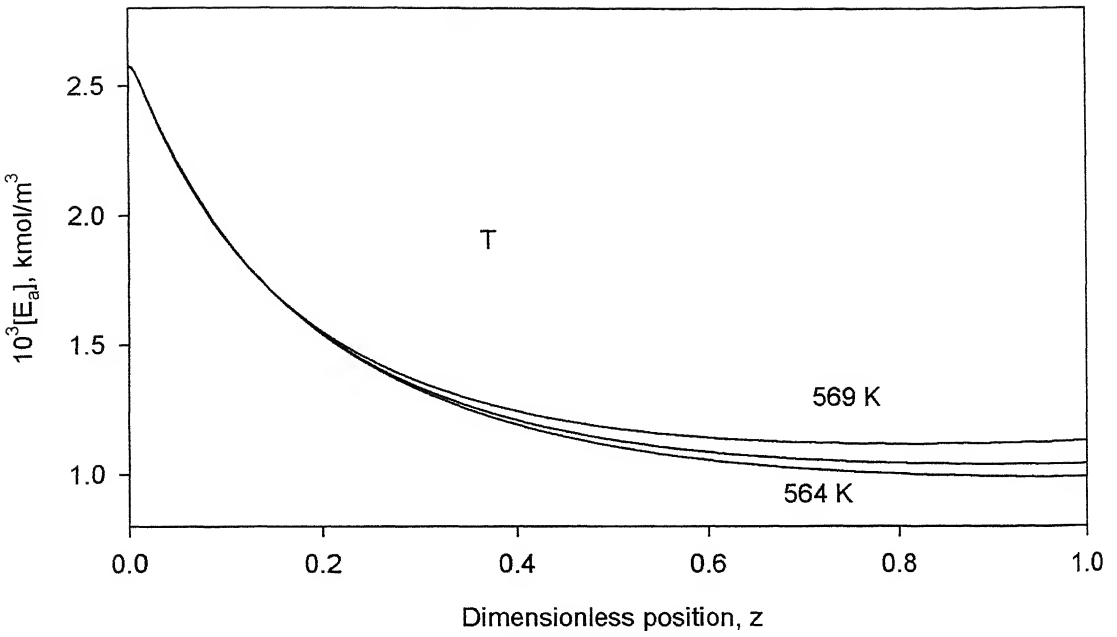

Figure. 2.3 Effect of temperature on the variation of the acid end group concentration, $[E_a]$, with z. The unmarked curve corresponds to 566 K.

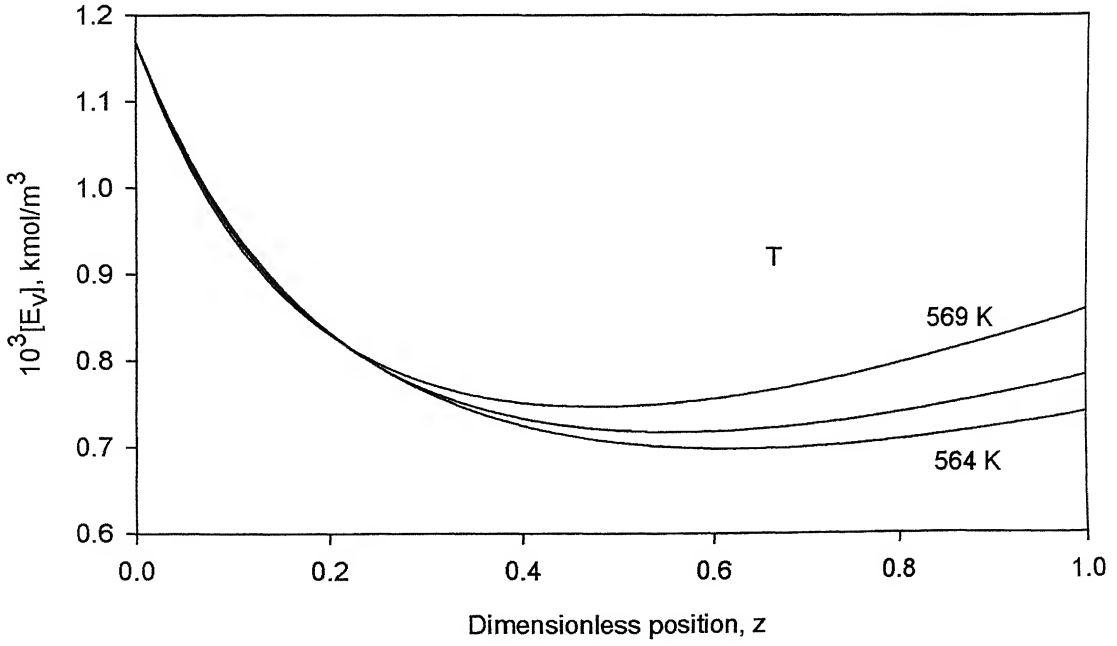

Figure. 2.4 Effect of temperature on the variation of the vinyl end group concentration, $[E_v]$, with z. The unmarked curve corresponds to 566 K.

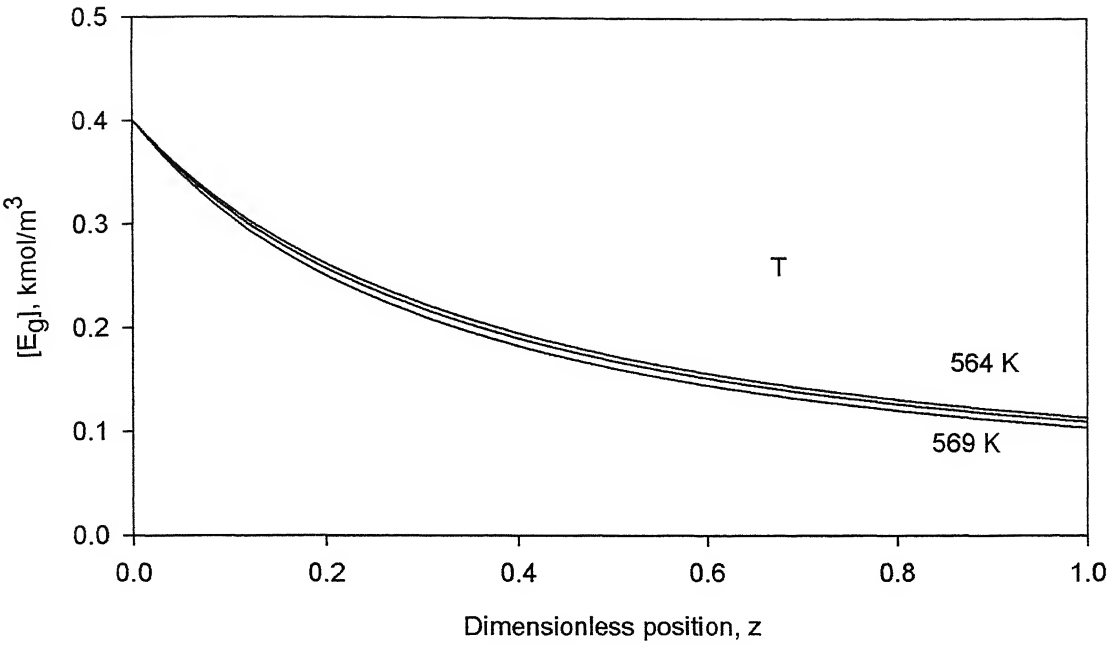

Figure. 2.5 Effect of temperature on the variation of the hydroxyl end group concentration, $[E_g]$, with z. The unmarked curve corresponds to 566 K.

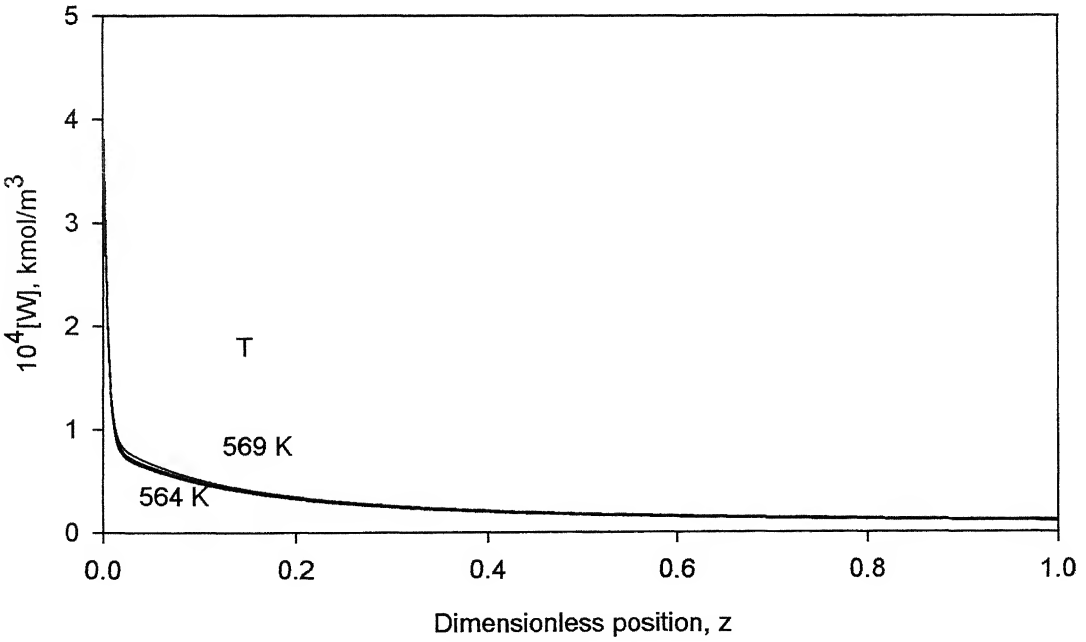

Figure. 2.6 Effect of temperature on the variation of the water concentration, [W], with z. The unmarked curve corresponds to 566 K.

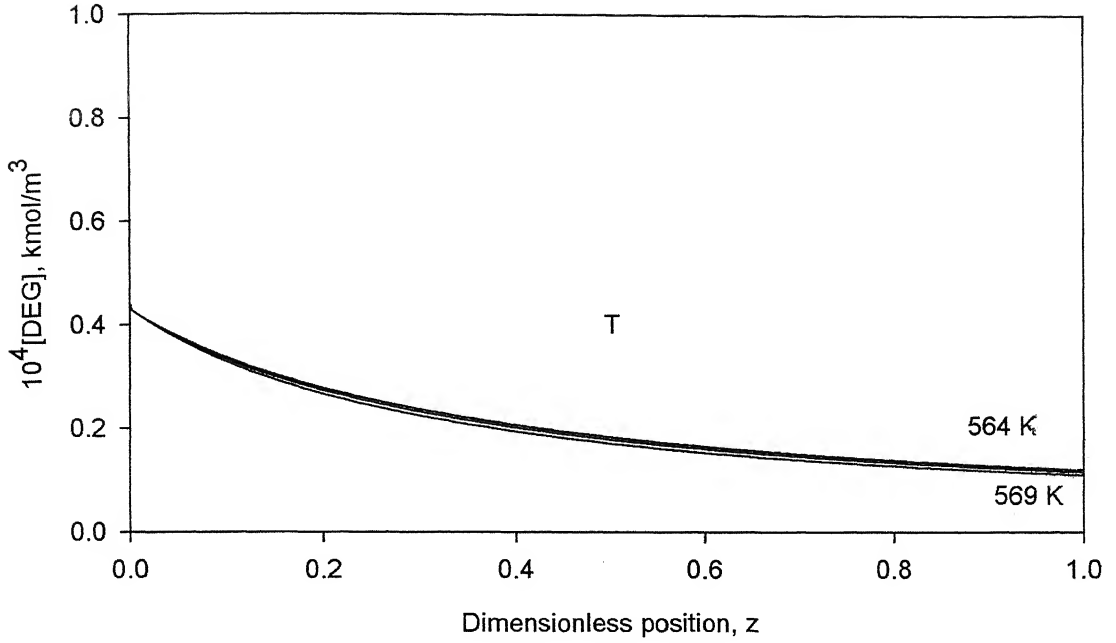

Figure. 2.7 Effect of temperature on the variation of the DEG concentration, [DEG], with z. The unmarked curve corresponds to 566 K.

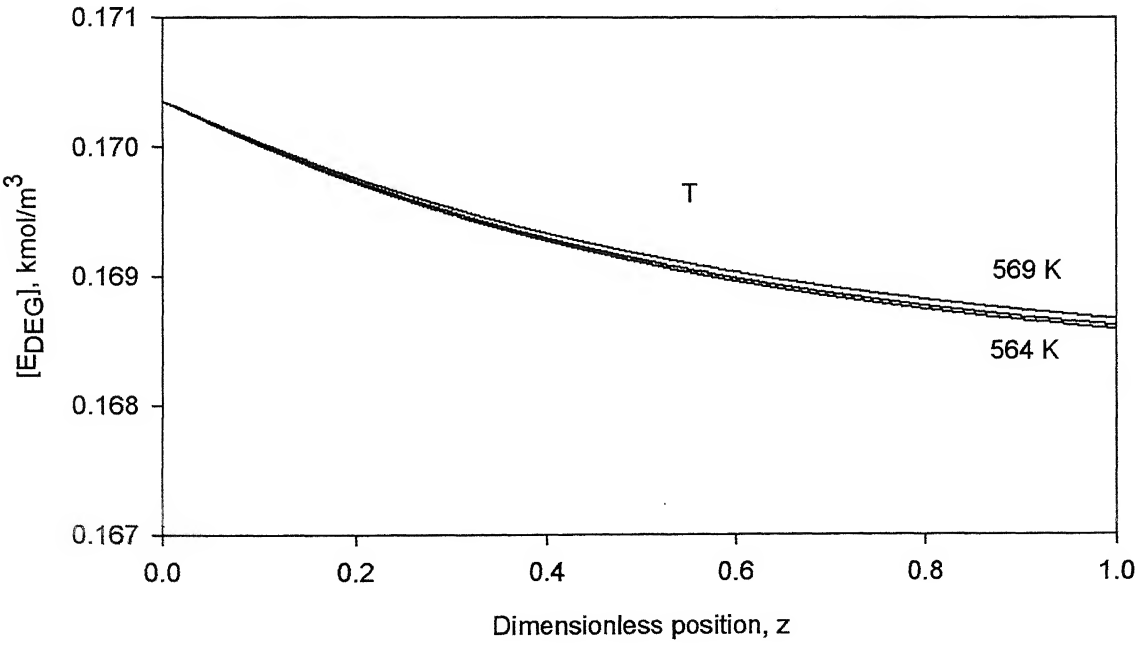

Figure. 2.8 Effect of temperature on the variation of the DEG end groups concentration, [E_{DEG}], with z. The unmarked curve corresponds to 566 K.

of $[E_a]$, which is known to affect the hydrolytic stability of the polymer product. High concentrations of $[E_a]$ lead to problems during the spinning and drawing stages in fiber manufacture due to the use of moist air and water in these operations. Lower temperatures also favor lower values of $[E_v]$. Fig. 2.8 shows that increasing temperatures leads to higher concentrations of E_{DEG} at the outlet of the reactor. This is in contrast to the trend observed for the concentration of the volatile species, DEG, the concentration of which is far lower due to its vaporization. The increase of $[E_{DEG}]$ with increasing temperatures is, indeed, observed for the industrial reactor being studied, and is opposite to the effect observed by Laubriet et al. (1991). The concentration of E_{DEG} in the final polymer determines its degree of crystallinity and hence its dyeability, and it is important to have a model, which predicts the right trends. Table 2.7 summarizes the effects of varying the different operating conditions and parameters on the values of the concentrations of the various side products, as well as the DP at the outlet of the reactor. It is observed that the pressure in the reactor has a strong influence on the DP of the product. The DP of the polymer at the reactor outlet increases from about 82.07 to 84.06 as the pressure decreases from 2.0 to 0.5 mm Hg. Decreasing pressures facilitate the removal of EG from the bulk melt phase and enhance the growth of the polymer chains. The concentration of DEG in the product decreases as the pressure is lowered. This effect is similar to what happens with increasing temperatures. The value of $[E_a]$ is not affected much by changing pressures, in sharp contrast to the behavior with increasing temperatures. The effect of decreasing pressure on $[E_v]$ in the product is, again, much less than the effect of temperature. It is clear that lower pressures are used to produce higher molecular weight polymer since they compensate the effects of lower temperatures that are required to keep the other product properties within prescribed limits. These trends would be useful in optimization studies in the future.

Table 2.7 shows that the DP of the final product increases as the residence time is increased. This is associated with a faster depletion of hydroxyl end groups. The other side product concentrations are not affected much by a change in the residence time. Again, one would like to minimize the residence time in any optimization study, while producing polymer having the same values of DP, thereby increasing the throughput. Table 2.7 shows that while a_o, the value of χ_1 at the feed end of the reactor does not influence the DP of the product much, b_o does, indeed, have some effect. b_o is also seen to affect the value of $[E_{DEG}]$. Though the tuned values of a_o and b_o were able to predict the industrial results fairly well, the sensitivity of DP and $[E_{DEG}]$ to b_o suggests the importance of obtaining better correlations for χ_1.

An increase in k_La_{ref} leads to increasing values of DP, while it decreases $[E_a]$, both being desirable objectives. The value of $[E_{DEG}]$ decreases with an increase in k_La_{ref}, which may not be desirable. An increase in k_La could be achieved by a better design of the agitator, an increase in the speed of the agitator, or by altering the level of the melt in the reactor. The first of these cannot be achieved except at the design stage. Lowering the level of the melt in the finisher simultaneously leads to an increase in the residence time, which counteracts the advantages attained because of lower rates of production. The manipulation of the agitator speed, N, is, therefore, a more preferred control-action in industry, particularly if the reduction of pressure is not sufficient to achieve an objective. In fact, a modification of pressure and/or the speed of the agitator are most often used for negating the effects of unplanned disturbances affecting the DP of the product in actual reactor operations.

An increase in the catalyst concentration from 0.03 or 0.0425% leads to a significant increase in both the DP of the product and vinyl end group concentration, the first desirable and second one undesirable attribute. Indeed, changes in the catalyst concentration and temperature

are used as the final recourse in industrial practice when changes in both pressure and the speed of the agitator are unable to negate the effect of disturbances on the DP of the polymer product. Unfortunately, the time lags associated with both these corrective control actions (catalyst concentration and temperature) are large, and this is why these actions are used only when the other means (pressure and the speed of the agitator) have failed.

The catalyst concentration also affects the color of the polymer produced. Barkley and Predmore (1970) and Chimaru et al. (1973) have suggested that the Sb^{3+} in the Sb_2O_3 catalyst gets reduced to metallic Sb^0 during the reaction. David and Lawrence (1995) have found experimentally that there is a non-linear dependence of the L-color (a measure of the luminosity or the whiteness) of the polymer on the concentration of Sb^0. In fact, increasing Sb_2O_3 concentrations leads to an undesirable greying of the polymer (lower L-color). Since our kinetic model does not incorporate this phenomenon, we should constrain the concentration of the catalyst so as to achieve a balance between the L-color and the two other properties of the polymer (DP and $[E_v]$), which are strongly influenced, by the catalyst concentration.

Since several rate and equilibrium constants have been 're-tuned' in this study to achieve a good fit, it is important to see the sensitivity of the results to these parameters. Table 2.7 shows that of the four equilibrium constants present in the reaction scheme, the DP of the polymer product is more significantly influenced by K_1 and K_5. An increase in K_5 also leads to a significant decrease in $[E_{DEG}]$. Indeed, K_5 was used as a tuning parameter in this study, primarily to achieve a better curve-fit of the industrial $[E_{DEG}]$ value. An increase in K_8 leads to a desirable lowering of the acid end group concentration. Table 2.7 also shows that increasing k_{2o} leads to an increase of the acid end group concentration, and an increase in k_{3o} leads to a significant decrease in $[E_v]$ and a small increase in DP of the polymer, while an increase in k_{9o} results in a decrease of DP but a *substantial* increase in $[E_a]$, $[E_v]$ and [W], which is highly undesirable. It is

clear from this sensitivity study that one needs to get better estimates for the rate and equilibrium constants using experimental data under more ideal reaction conditions, rather than from industrial data where several additional physical phenomena are present. It may be added that tuning of the rate and equilibrium constants to explain *industrial* data has been used for other polymerization systems as well, e.g., LDPE (Zabisky et al., 1992) and nylon 6 (Wajge et al., 1994).

2.4 Summary

An improved and re–tuned model for the finishing reactor in PET manufacture is developed. Optimal values of the parameters of the model are estimated using industrial data available with us. Data involving commercially important product properties like DP and the concentrations of the DEG and acid end groups have been used. The parameters tuned are $k_L a_{ref}$, the Flory-Huggins' interaction parameter, χ_1, the equilibrium constants, K_1, K_5 and K_8, the frequency factors of three-rate constants, k_2, k_3 and k_9, and α, a parameter associated with the effect of the rpm of the agitator on $k_L a$. These parameters are tuned using three sets of industrial data. The tuned parameters are then used unchanged to predict the concentration of the various side products and the DP for a different operating temperature. It is found that the model predicts these values very well. A sensitivity analysis is then performed using the tuned values of the model parameters, and the effect of several operating variables as well as parameters on the important physical properties is studied. Conflicting trends are observed from the model and insights developed can now be used to formulate and obtain meaningful solutions to problems on the optimization as well as control of this industrial reactor. This study brings out the importance of having accurate kinetic data, as well as of values of χ_1 and $k_L a$.

Chapter 3: INTRODUCTION TO NSGA - I AND NSGA -II

3.1 Genetic Algorithm (GA)

GA is a search technique developed by Holland (1975) that mimics the process of natural selection and natural genetics. In this algorithm, we code a set of values of the decision variables (a solution, x) in terms of a 'string (or chromosome)' of binary numbers, generated using random numbers. A 'population (gene pool)' of such binary strings is first generated. Each chromosome is then mapped into a set of *real* values of the decision variables, using the upper and lower bounds of each of these. This ensures that the decision variables lie within their bounds. Then, a model of the process is used to provide values of the objective function for each chromosome. The value of the objective function of any chromosome reflects its 'fitness'. The Darwinian principle of ' survival of the fittest' is used to generate a new and improved gene pool (new generation). This is done by preparing a 'mating pool', comprising of copies of chromosomes, the number of copies of any chromosome being proportional to its fitness (Darwin's principle). Pairs of chromosomes are then selected randomly, and pairs of daughter chromosomes generated using operations similar to those in genetic reproduction. The gene pool evolves, with the fitness improving over the generations.

GA is noted for its robustness. This algorithm is superior to traditional optimization algorithms in many aspects, and has become quite popular in recent years. It is better than calculus-based methods (both direct and indirect methods) that generally seek out the local optimum, and which may miss the global optimum. Most of the older techniques require values of the derivatives of the objective functions, and quite often, numerical approximations of the derivatives are used for optimization. In most real-life problems, the existence of derivatives is questionable and often, the functions are discontinuous, multi-modal and noisy. In such cases,

calculus-based methods fail. Enumerative schemes, which are based on the point-by-point comparison of the values of the objective function in a discretized infinite (or even a finite) search space, are inefficient for large problems since the search space is often, too large. Random search techniques, too, suffer from a similar disadvantage since they work like enumerative techniques in the long run. GA is superior to these techniques since it is conceptually different from these traditional algorithms in several respects. It uses a population of several points simultaneously, as well as works with probabilistic (instead of deterministic) operators. In addition, GA uses information on the objective function and not its derivatives, nor does it require any other auxiliary knowledge.

Three common operators are used in GA [called simple GA (SGA), to distinguish it from its various adaptations] to obtain an improved (next) generation of chromosomes. These are referred to as reproduction, cross-over and mutation. Reproduction, as described above, is the generation of the mating pool, where the chromosomes are copied probabilistically, based on their fitness values. Then, a pair of daughter chromosomes are produced by selecting a cross-over site (chosen randomly) and exchanging the two parts of the pair of parent chromosomes (selected randomly from the mating pool), as illustrated below for two chromosomes carrying information about three decision variables, each represented by four binary digits:

1001 1¦100 0111		1001 1¦191 1100	
0011 0¦101 1100	$\Rightarrow$	0011 0¦100 0111	(3.1)
Parent chromosomes		Daughter chromosomes	

In Eq. 3.1, the crossover site for *this* pair of parent chromosomes is taken just after the fifth binary digit. It is hoped that the daughter strings are superior. If they are worse than the parent

chromosomes, they will slowly die a natural death over the next few generations (the Darwinian principle at work).

The mutation operator is required for the following reason. In Eq. 3.1, let us assume that *all* the chromosomes in the gene pool have a 0 at the second position. There is a finite probability of this happening, since the generation of the binary numbers is done probabilistically. It is obvious that cross-over will never be able to generate chromosomes with a 1 at this position, and if it so happens that the optimum is, indeed, located at a point described by such a chromosome, GA will be unable to reach this solution. The mutation operator looks at *each* binary digit in *every* daughter chromosome in the gene pool, and transforms a 0 into a 1 (or vice versa) with a small probability. In effect, it moves the chromosome *locally* in the **x**-space, to create a better chromosome. The entire process is repeated till some termination criterion is met (the specified maximum number of generations is attained, or the improvements in the values of the objective functions become lower than a specified tolerance). A more elaborate description of SGA is available in Holland, 1975, Goldberg, 1989, and Deb, 1995.

3.2 NSGA - I (Nondominated Sorting Genetic Algorithm - I)

SGA has been extended to solve problems involving multiple objectives. Since GA uses a population of points, it seems very natural to use GA for such problems to capture a number of solutions *simultaneously.* Schaffer (1984) was the first to apply an adapted Vector Evaluated Genetic Algorithms (VEGA) to solve multiobjective optimization problems. Though it was simple to implement, the method has a bias towards some Pareto-optimal solutions (Goldberg, 1989; Srinivas and Deb, 1995). In order to overcome this problem of bias with some of the optimal solutions, Goldberg proposed a non-dominated sorting procedure. The idea was implemented in different ways by Fonseca and Fleming (1993), Horn et al. (1994) and Srinivas

and Deb (1995). The algorithm implemented by Srinivas and Deb (1995) is called the non-dominated sorting genetic algorithm (NSGA - I). It is to be noted that NSGA - I overcomes the pitfalls of the previous two techniques (Fonseca and Fleming, 1993, Horn et al. 1994). Fonseca and Fleming (1998 a,b) have recently extended their algorithm, applying the principles of niche and sharing.

NSGA – I uses a ranking selection method to emphasize the good points and a niche method to create diversity in the population without losing a stable sub-population of good points. Principally, NSGA – I differs from SGA *only* in the way of selection. A check for non-dominance is first carried out among *all* the chromosomes in the gene pool before reproduction is performed. All the non-dominated chromosomes from the entire population are first identified and assigned a front number (Front No. = 1). These non-dominated chromosomes are then assigned a *dummy* fitness value (which is usually the number of chromosomes, N_p, but could be any other arbitrarily selected large value instead). The dummy fitness value of any chromosome in this front is then modified according to a sharing procedure (Goldberg and Richardson, 1987; Deb, 1989; Deb and Goldberg, 1991) by dividing it by the niche count of the chromosome. The niche count of a chromosome represents the number of neighbors around it, with distant neighbors contributing less than those nearby. The niche count, thus, gives an idea of how crowded the chromosomes are in the **x**-space. This is obtained, say, for the i^{th} chromosome, by computing its distance, d_{ij}, from another, say, j^{th} chromosome in the **x**-space, and using a sharing function, Sh, as given below

$$Sh(d_{ij}) = 1 - \left(\frac{d_{ij}}{\sigma_{share}} \right)^{\alpha}, \text{ If } d_{ij} < \sigma_{share} \text{ ; 0, otherwise} \qquad (3.2)$$

In Equation 3.2, σ_{share}, a computational parameter, is the maximum distance allowed between two chromosomes to qualify as neighbors. Obviously, if d_{ij} is larger than σ_{share}, its contribution to Sh is zero (the j^{th} chromosome is then not considered to be a neighbor of the i^{th}), while if $d_{ij} = 0$, its contribution to Sh is 1. For intermediate values of the distance between the two chromosomes, Sh lies between 0 and 1. Thus, by summing up Sh (d_{ij}) for *all values of* j in any front comprising of non-dominated chromosomes, one can get an idea of how crowded the i^{th} chromosome really is. This summation is referred to as the niche count of chromosome i. The shared fitness value of chromosome i is the ratio of the common dummy fitness value assigned initially to each member of the front, and its niche count. Use of the shared fitness value for reproduction, thus, helps spread out the chromosomes in the front since crowded chromosomes are assigned lower fitness values. This procedure is repeated for all the members of the first front. Once this is done, these chromosomes are temporarily removed from consideration, and all the *remaining* ones are tested for non-dominance. The non-dominated chromosomes in *this* round are classified into the next front (Front No. = 2). These are all assigned a dummy fitness value that is a bit lower than the *lowest* shared fitness value of the previous front. Sharing is performed thereafter. This procedure is continued till all the chromosomes in the gene pool are assigned shared fitness values. The usual operations of reproduction, cross-over and mutation are now performed. It is clear that the non-dominated members of the first front that have fewer neighbors, will get the highest representation in the mating pool. Members of later fronts, which are dominated, will get lower representations (they are still assigned some low fitness values, rather than 'killed', in order to maintain the diversity of the gene pool). Sharing forces the chromosomes to be spread out in the **x**-space. The population is found to converge very rapidly to the Pareto set. It is to be noted that any number of objectives (both minimization and maximization problems) can be solved using

Figure 3.1: A flowchart of the adapted NSGA - I*

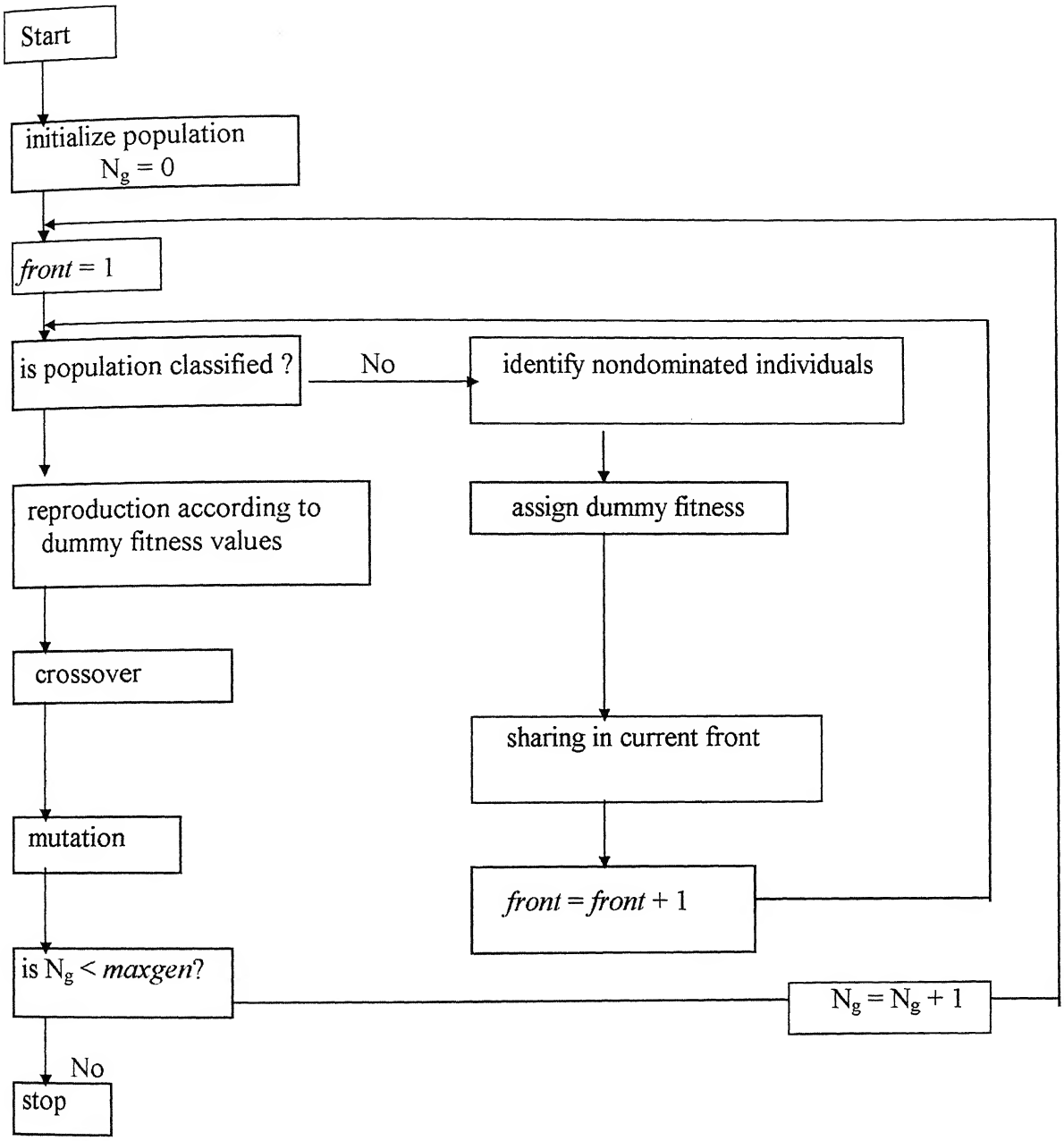

*From Mitra et al. (1998) and Garg and Gupta (1999).

this procedure. A flowchart describing this technique is presented in Figure 3.1 (Mitra et al., 1998; Garg and Gupta, 1999). Additional details about the algorithm, its efficiency over other techniques and some comments on the choice of the computational parameters to be used in NSGA - I, are described in Srinivas and Deb, 1995 and Deb, 1989.

3.3 NSGA – II (*Elitist* Non-dominated Sorting Genetic Algorithms - II)

Over the years, the main criticisms of the NSGA - I proposed by Srinivas and Deb(1995) have been :

High computational complexity of non-dominated sorting: The currently-used non-dominated sorting algorithm has a computational complexity of $O(MN^2)$ (where M is the number of objectives and N is the population size). This makes NSGA–I a computationally intensive algorithm for large population sizes. This large complexity arises because of the complexity involved in the non-dominated sorting procedure in every generation.

Lack of elitism: Recent results show clearly that elitism can speed up the performance of GA significantly. Also, it can help preventing loss of good solutions once they are found.

Need for specifying the sharing parameter, σ_{share}*:* Traditional mechanisms of ensuring diversity in a population so as to get a wide variety of equivalent solutions have relied mostly on the concept of sharing. The main problem with sharing is that it requires the specification of a sharing parameter (σ_{share}). Though there has been some work on dynamic sizing of the sharing parameter, a parameter-less diversity preservation mechanism is desirable. An improved version of NSGA, called NSGA – II (*Elitist* non-dominated sorting genetic algorithm) alleviates all the above three difficulties. A number of different modules that form parts of NSGA – II are presented below:

A. A Fast Non-dominated Sorting Approach

In NSGA – I, in order to sort a population of size N according to the level of non-domination, each solution must be compared with every other solution in the population to find if it is dominated. This requires $O(MN)$ comparisons for each solution, where M is the number of objectives. When this process is continued to find the members of the first non-dominated class for all population members, the total complexity is $O(MN^2)$. At this stage, all individuals in the first non-dominated front are found. In order to find individuals of the next front, the solutions of the first front are temporarily discounted and the above procedure is performed again. The procedure is repeated to find subsequent fronts. As can be seen, the worst case (when there exists only one solution in each front) the complexity of this algorithm without any book-keeping is $O(MN^3)$. In the following, we describe a fast non-dominated sorting approach which will require at most $O(MN^2)$ computations.

This approach ensures a better book-keeping strategy to make it a faster algorithm. In this approach, every solution from the population is checked with a *partially filled* population for domination. To start with, the first solution from the population is kept in a set P'. Thereafter, each solution, p (the second solution onwards) is compared with all members of the set P', one by one. If the solution, p, dominates any member q of P', then solution q is removed from P'. In this way, non-members of the non-dominated front get deleted from P'. Otherwise, if solution p is dominated by any member of P', solution p is ignored. If solution p is not dominated by any member of P', it is entered in P'. This is how the set P' grows with non-dominated solutions. When all solutions of the population have been checked, the remaining members of P' constitute the non-dominated set.

Here, we observe that the second population member is compared with only one solution of P', the third solution with at most two solutions of P', and so on. This requires a maximum of $O(N^2)$ domination checks. Since each domination check requires M function value comparisons, the maximum complexity of this approach to find the first non-dominated front is also $O(MN^2)$.

To find other fronts, the members of P' will be discounted from P and the above procedure is repeated.

3. *Diversity Preservation*

NSGA – I uses the well-known sharing function approach, which has been found to maintain sustainable diversity in a population with appropriate setting of its associated parameters. The sharing function method involves a sharing parameter, σ_{share}, which sets the extent of sharing desired in a problem. This parameter is related to the distance metric chosen to calculate the proximity measure between two population members. The parameter, σ_{share}, denotes the largest value of that distance metric within which any two solutions share each other's fitness. The user usually sets this parameter. There are two difficulties with this sharing approach:

1. The performance of the sharing function method in maintaining a spread of solutions largely depends on the chosen value of σ_{share}.
2. Since each solution must be compared with all other solutions in the population, the overall complexity of the sharing function approach is $O(N^2)$.

In NSGA - II , the sharing function approach is replaced with a crowded comparison approach which eliminates both the above difficulties to some extent. This approach

does not require *any* user-defined parameter for maintaining diversity among population members. Also, the suggested approach is better in terms of computational complexity. To describe this approach, we first define a density estimation metric and then present the crowded comparison operator.

B.1 Density Estimation

To get an estimate of the density of solutions surrounding a particular solution in the population, we calculate the average distance of two points on either side of this point along each of the objectives. This quantity, $i_{distance}$, serves as an estimate of the size of the largest cuboid enclosing any point, I, without including any other point in the population (we call this the *crowding distance*).

The crowding distance computation requires sorting of the population according to the value of each objective function in their ascending order of magnitude. Thereafter, for each objective function, the boundary solutions (solutions with smallest and largest function values) are assigned an infinite distance value. All other intermediate solutions are assigned a distance value equal to the absolute difference in the function values of two adjacent solutions. This calculation is continued with other objective functions. The overall crowding distance value is calculated as the sum of individual distance values corresponding to each objective. The complexity of this procedure is governed by the sorting algorithm. Since M independent sorting of at most N solutions (when all population members are in one front) are involved, the above algorithm has a computational complexity of $O(MN \log N)$.

After all members of the population in the set are assigned a distance metric, we can compare two solutions for their extent of proximity with other solutions. A solution with a

smaller value of this distance measure is, in some sense, more crowded than other solutions. This is exactly what we compare in the proposed crowded comparison operator, described below.

B.2 Crowded Comparison Operator

The crowded comparison operator ($\prec_n$) guides the selection process at the various stages of the algorithm towards a uniformly spread-out Pareto-optimal front. Let us assume that every individual *i* in the population has two attributes:

1. non-domination rank (i_{rank}), and
2. crowding distance ($i_{distance}$).

We now define a partial order, $\prec_n$, as :

$$i \prec_n j \text{ if } (i_{rank} < j_{rank}) \text{ or } [(i_{rank} = j_{rank}) \text{ and } (i_{distance} > j_{distance})]$$

That is, between two solutions with differing non-domination ranks we prefer the solution with the lower (better) rank. Otherwise, if both solutions belong to the same front, then we prefer the solution which is located in a lesser-crowded region.

With these three new innovations – a fast non-dominated sorting procedure, a fast crowded distance estimation procedure, and a simple crowded comparison operator, we are now ready to describe NSGA –II.

C. The Main Loop

Initially, a random parent population, P_0, is created. The population is sorted based on non-domination. Each solution is assigned a fitness (or rank) equal to its non-domination level (1 is the best level, 2 is the next-best level, and so on). Thus, minimization of fitness

is assumed. At first, the usual binary tournament selection, recombination, and mutation operators are used to create a child population Q_0 of size N. Since elitism is introduced by comparing the current population with the previously found best non-dominated solutions, the procedure is different after the initial generation. A flowchart of a generation of NSGA – II is given in Fig. 3.2.

First, a combined population, $R_t = P_t \cup Q_t$, is formed. The population, R_t, will be of size 2N. Then, the population R_t is sorted according to non-domination. Since all previous and current population members are include in R_t, elitism is ensured. Now, solutions belonging to the best non-dominated set, f_1, are the best solutions in the combined population and must be emphasized more than any other solution in the combined population. If the size of f_1 is smaller than N, we definitely choose all members of the set, f_1, for the new population, P_{t+1}. The remaining members of the population, P_{t+1}, are chosen from subsequent non-dominated fronts in the order of their ranking. Thus, solutions from the set f_2 are chosen next, followed by solutions from the set f_3, and so on. This procedure is continued till no more sets can be accommodated. Let us say that the set, f_l, is the last non-dominated set beyond which no other set can be accommodated. In general, the count of solutions in all sets from f_1 to f_l would be larger than the population size. To choose exactly N population members, we sort the solutions of the last front using the crowded comparison operator, $\prec_n$, in the descending order and choose the best solutions needed to fill all the population slots. The new population, P_{t+1}, of size N is now used for selection, crossover and mutation to create a new population, Q_{t+1}, of size N. It is important to note that we use a binary tournament selection operator but the selection criterion is now based on the crowded comparison operator, $\prec_n$. Since this operator requires both the rank and crowded

Figure 3.2 : Flowchart of a generation of NSGA-II

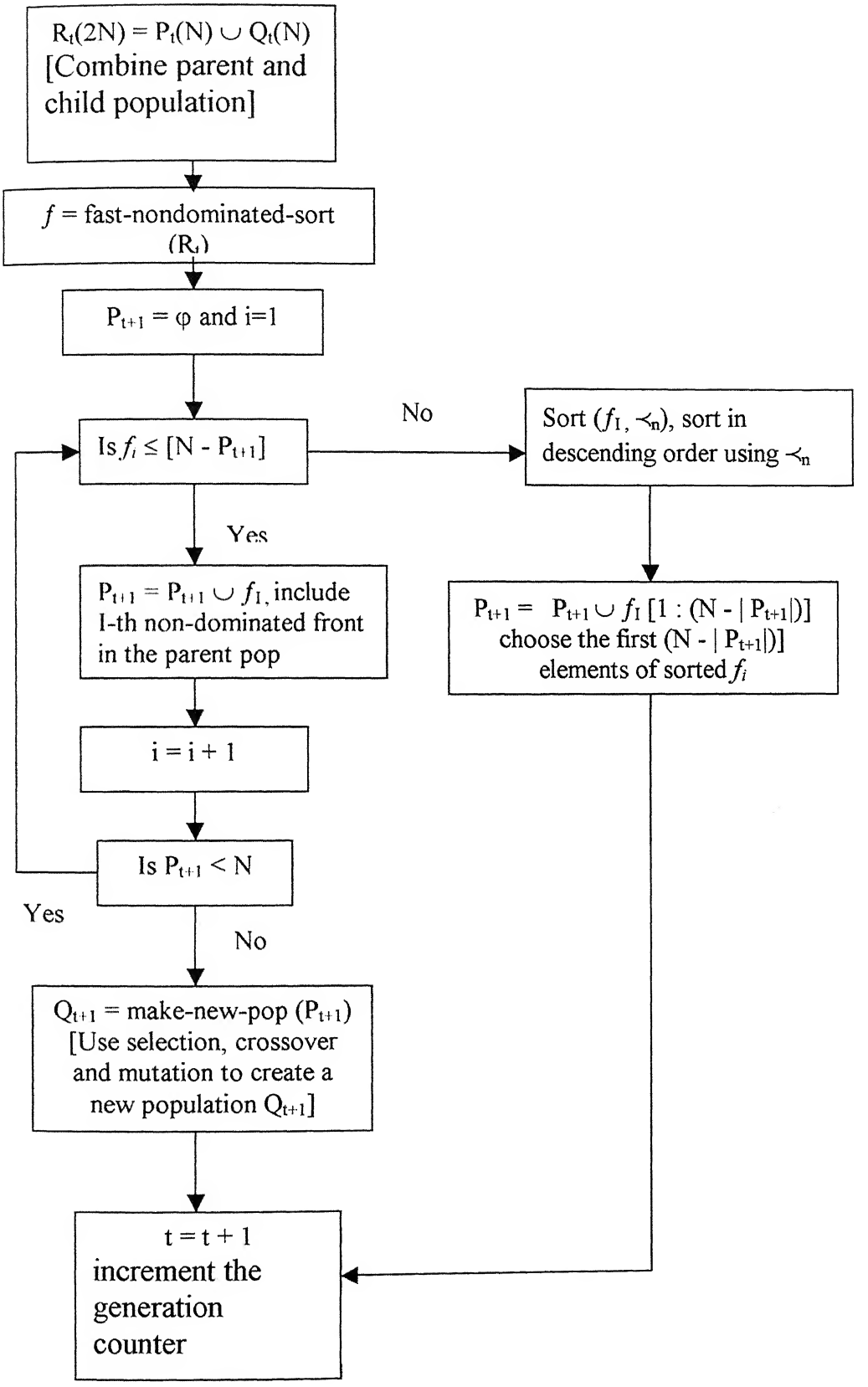

distance of each solution in the population, we calculate these quantities while forming the population, P_{t+1}.

Let us now look at the complexity of one iteration of the entire algorithm. The basic operations and their worst-case complexities are as follows:

1. Non-dominated sorting is $O[M(2N)^2]$,
2. Crowding distance assignment is [M(2N)log (2N)], and
3. Sorting on $\prec_n$ is O[2Nlog(2N)].

As can be seen, the overall complexity of the above algorithm is $O(MN^2)$, which is governed by the non-dominated sorting part of the algorithm.

The diversity among non-dominated solutions is introduced by using the crowding comparison procedure, which is used in the tournament selection and during the population reduction phase. Since solutions compete with their crowding distance (a measure of density of solutions in the neighborhood), no extra niche parameter (such as σ_{share} needed in NSGA – I) is required here. Although the crowding distance is calculated in the objective function space, it can also be implemented in the parameter space, if so desired.

3.3 Summary

In this section, we discussed the use of genetic algorithms for solving multiobjective optimization problems. Two adaptations of the genetic algorithm, NSGA – I and NSGA – II, were discussed and the flowchart describing each is presented. In the next section, multiobjective optimization of the finishing reactor under consideration is discussed.

Chapter 4: MULTIOBJECTIVE OPTIMIZATION OF THE FINISHING REACTOR

4.1 Introduction

Process industries aim at maximizing their production capacities while simultaneously maintaining the product quality. Usually, there exists a trade-off between these two requirements. This is particularly true in the manufacture of polymers where the properties of the product are crucial and reactors have to be operated under conditions which yield products that satisfy relatively narrow specifications. At the same time, the operating variables must be at their optimal conditions to maximize the throughput. It is well established that the average molecular weight of the polymer produced determines several important physical properties of the material, e.g., strength, impact resistance, etc. In addition, the concentrations of a few side products need to be below low limits or between narrow limits to ensure some other properties like color, dyeability, etc., to lie within specifications. Thus, the design and operation of polymerization reactors require optimization using multiple objective functions and constraints, which are often conflicting. A multiobjective optimization problem was formulated for the finishing reactor in the polyethylene terephthalate manufacture and the problem was solved using two adaptations of GA, NSGA – I and NSGA – II.

4.2 Problem Formulation

The two important objective functions for this system are the minimization of the acid and the vinyl end group concentrations, $[E_a]_{out}$ and $[E_v]_{out}$, respectively, in the product of the finisher. The acid end group makes the polymer susceptible to hydrolysis [Besnoin and Choi (1989)] during the downstream operations and leads to breakage of the filaments during spinning, where the humidity is very high. The vinyl end groups have been shown to be

responsible for the coloration of PET [Besnoin and Choi (1989), James and Packer (1995)] because of reactions not well understood right now, and not included in Table 2.1. Hence, the minimization of these two end groups improves the quality of the polymer product. The reduction of $[E_a]_{out}$ simultaneously increases the rate of polymerization of the acid end group catalyzed polycondensation reaction and helps maximize the throughput (this catalytic effect is not *directly* incorporated in the model, however). The important end-point constraint is to produce polymer having a desired value of the degree of polymerization (DP). Though the diethylene glycol (DEG) end groups affect the crystallinity and hence the melting point of the polymer unfavorably, they do improve the dyeability of the fiber. Therefore, it is preferred to have a certain allowable *range* for the concentration of DEG end groups in the fiber-grade polyesters. An inequality constraint is, therefore, imposed for the DEG end group concentration in the product, as per industrial requirements. In addition, a further inequality constraint on the maximum allowable limit for the acid end group concentration is imposed to ensure that it is not only minimized, but also lies below an upper limit. Five decision variables are used for optimization in this study. These are: the reactor pressure (P), temperature (isothermal, T), catalyst concentration ($[Sb_2O_3]$), residence time of the polymeric reaction mass inside the reactor (θ) and the speed of the wiped-film agitator (N). All of these variables can easily be changed in any industrial, wiped film reactor for PET manufacture, including the one being studied, and are, therefore, used to obtain the best optimal operating conditions.

The multiobjective function optimization problem described above and studied in this work is, thus, described mathematically by [Bhaskar et al. (2000b)]:

$$\text{Min } \boldsymbol{I}\ (P, T, [Sb_2O_3], \theta^*, N^*) \equiv [I_1, I_2]^T = [[E_a]_{out}, [E_v]_{out}]^T \qquad (4.1a)$$

subject to (s. t.)

$$DP_{out} = DP_d \tag{4.1b}$$

$$[E_a]_{out} \leq 1.038 \times 10^{-3} \text{ kmol/m}^3 \tag{4.1c}$$

$$0.1660 \leq [E_{DEG}]_{out} \leq 0.17 \text{ kmol/m}^3 \tag{4.1d}$$

$$dx/dz = f(x,u); \qquad x(z=0) = x_0 \tag{4.1e}$$

Bounds:

$$0.05 \leq P \leq 0.266 \text{ kPa } (0.4 \leq P \leq 2.0 \text{ mm Hg}) \tag{4.1f}$$

$$564 \leq T \leq 570 \text{ K} \tag{4.1g}$$

$$0.03 \leq [Sb_2O_3] \leq 0.045 \text{ wt\%} \tag{4.1h}$$

$$0.90 \leq \theta^* \leq 1.06 \tag{4.1i}$$

$$0.93 \leq N^* \leq 1.05 \tag{4.1j}$$

where the subscripts 'out' and 'd' refer to the values at the outlet of the reactor and the desired values of the product property, respectively. The variables, θ^* and N^*, represent dimensionless values, θ/θ_{ref} and N/N_{ref}, where θ_{ref} and N_{ref} are the values being used currently in the industrial reactor being studied. These two values are confidential and are not being provided here due to proprietary reasons. Meaningful bounds have been chosen on the five decision variables, $\boldsymbol{u}$, based on industrial practice. These are given in Eqs. 4.1f-j. The mathematical model for the present study, the parameters and the other variables and details have already been presented in Chapter 2. In general, the state variable equations describing the reactor can be written in the form

$$dx/dz = f(x,u); \qquad x(z=0) = x_0 \tag{4.2}$$

where $\boldsymbol{x}$ is the vector of state variables, given by

$$\boldsymbol{x} = [\ [E_g], [E_a], [Z], [E_v], [E_{DEG}], [EG], [W], [DEG]\ ]^T \tag{4.3}$$

and $\boldsymbol{u}$ is the vector of decision variables given in Eq. 4.1 a.

The end-point constraint on DP in Eq. 4.1b is incorporated in the form of a penalty function (with $w_2 = 10^8$), in the two objective functions as follows:

$$Min \quad I_1^* = w_1 \, [E_a]_{out} + w_2 \left(1 - \frac{DP_{out}}{DP_d}\right)^2 + P_e \tag{4.4a}$$

$$Min \quad I_2^* = w_3 \, [E_v]_{out} + w_2 \left(1 - \frac{DP_{out}}{DP_d}\right)^2 + P_e \tag{4.4b}$$

An additional large 'penalty' value, P_e (used as 10^4 in this study), is added to the objective functions, I_1* and I_2*, if either of the two inequality constraints (Eqs. 4.1c and 4.1d), the maximum limit of the acid end group concentration at the outlet of the reactor, $[E_a]_{out}$, and the upper and lower bounds on the DEG end group concentration at the outlet of the reactor, $[E_{DEG}]_{out}$, are violated. If these constraints are satisfied, then the value of P_e in Eq. 4.4 is taken as zero. This ensures that bad chromosomes in the genetic algorithm used for optimization do not get reproduced in the successive generations even if several chromosomes violating these constraints exist in the initial population (i.e., chromosomes violating Eqs. 4.1c and 4.1d die out rapidly). Also, a very large value of P_e is added *if* the concentrations of three of the vaporizing species, EG, W and DEG in the vapor phase are higher than their respective vapor-liquid interfacial equilibrium concentrations, EG*, W* and DEG*, at any axial location. This ensures vaporization (rather than condensation) of these species at *all* axial locations. Minimization of I_1* and I_2* leads to a decrease in the acid end group concentration and the vinyl end group concentration in the product, while simultaneously giving preference to solutions satisfying the several requirements discussed above. The use of a penalty to 'kill' chromosomes when important physical constraints are violated is one of the several adaptations of the basic algorithm used in this study [Bhaskar et al. (2000)]. Use of w_1 and w_3 as 10^4 leads to values of

$w_1[E_a]_{out}$ and $w_3[E_v]_{out}$ of the order of unity. These two objective functions are conflicting in nature [Bhaskar et al. (2000b)]. Use of these is, thus, expected to lead to Pareto optimal solutions.

4.3 Results and Discussion

The solution of the multiobjective optimization problem described in Eq. 4.1 is obtained using both NSGA – I and NSGA - II, using values of the computational parameters and bounds of the decision variables, as given in Table 4.1. The value of DP_d was taken as 82.00, the value corresponding to the reference case for the industrial reactor simulated earlier. Such a study would help explore if changes in the operating variables could improve the performance of the industrial reactor. Figs. 4.1 and 4.2 show all the feasible solutions (i.e., those satisfying the end point constraints in Eqs. 4.1b-d) at different values of the generation number, N_g, when NSGA – II is used. In the initial generations, the feasible points are quite scattered in the $[E_a]_{out}$ - $[E_v]_{out}$ space, but as the chromosomes evolve over the generations, the feasible points move towards a unique point. There are 100, almost indistinguishable points in Fig. 4.3 (N_g = 100). The unique solution of our multiobjective function optimization problem with end-point constraints (using NSGA – II) is given by

$$\begin{aligned} [E_a]_{out} &= 9.58 \times 10^{-4}\ \text{kmol/m}^3 \\ [E_v]_{out} &= 7.392 \times 10^{-4}\ \text{kmol/m}^3 \\ DP_{out} &= 82.000 \end{aligned} \qquad (4.5)$$

Table 4.2 shows the values of the five decision variables corresponding to this optimal point (reference run), as well as corresponding values of several other product characteristics under the optimal operating condition.

Table 4.1: Computational variables used in this study

Weightage factors:

$w_1 = w_3 = 10^4$; $w_2 = 10^8$; $P_e = 10^4$

GA Parameters:

N_{gen} = 100 N_p = 100

p_c = 0.90 p_m = 0.001

l_{chrom} = 160 bits Sr = 0.3219 (NSGA – II), 0.6237 (NSGA – I)

Initial guess values used for y_i:

y_{EG} : 0.93

y_W : 0.0269

y_{DEG} : 0.0246

Variables/units	Lower bound	Upper bound	Reference value
P, kPa (mm Hg)	0.0532(0.4)	0.266(2.0)	0.266(2.0)
T (K)	564.00	570.00	564.15
$[Sb_2O_3]$ (wt.%)	0.03	0.045	0.04
θ^*	0.90	1.06	1.00
N^*	0.93	1.05	1.00

Table 4.2: Optimal operating conditions and product properties *

Operating conditions	Optimal (NSGA - II)	Optimal (NSGA – I)	Industrial	Bhaskar et. al.
P, kPa (mm Hg)	0.0754 (0.5674)	0.1787 (1.3441)	0.266 (2.0)	0.185 (1.39)
T, K	564.05	564.11	566.0	564.02
$10^{2}[Sb_2O_3]$, wt%	3.67	4.02	4.0	4.26
θ*	1.0350	0.9940	1.0	0.9672
N*	0.9929	1.0201	1.0	1.0
Product properties				
DP_{out}	82.00	82.00	82.00	82.00
$[E_g]_{out}$, kmol/m^3	0.1110	0.1102	0.1091	0.1101
$10^{4}[E_a]_{out}$, kmol/m^3	9.58	9.78	10.38	10.00
$10^{4}[E_v]_{out}$, kmol/m^3	7.39	7.50	7.8	7.5
$[E_{DEG}]_{out}$, kmol/m^3	0.1675	0.1681	0.1692	0.1682

* All the values given above are for $DP_d = 82.0$ and $DP_f = 40.0$

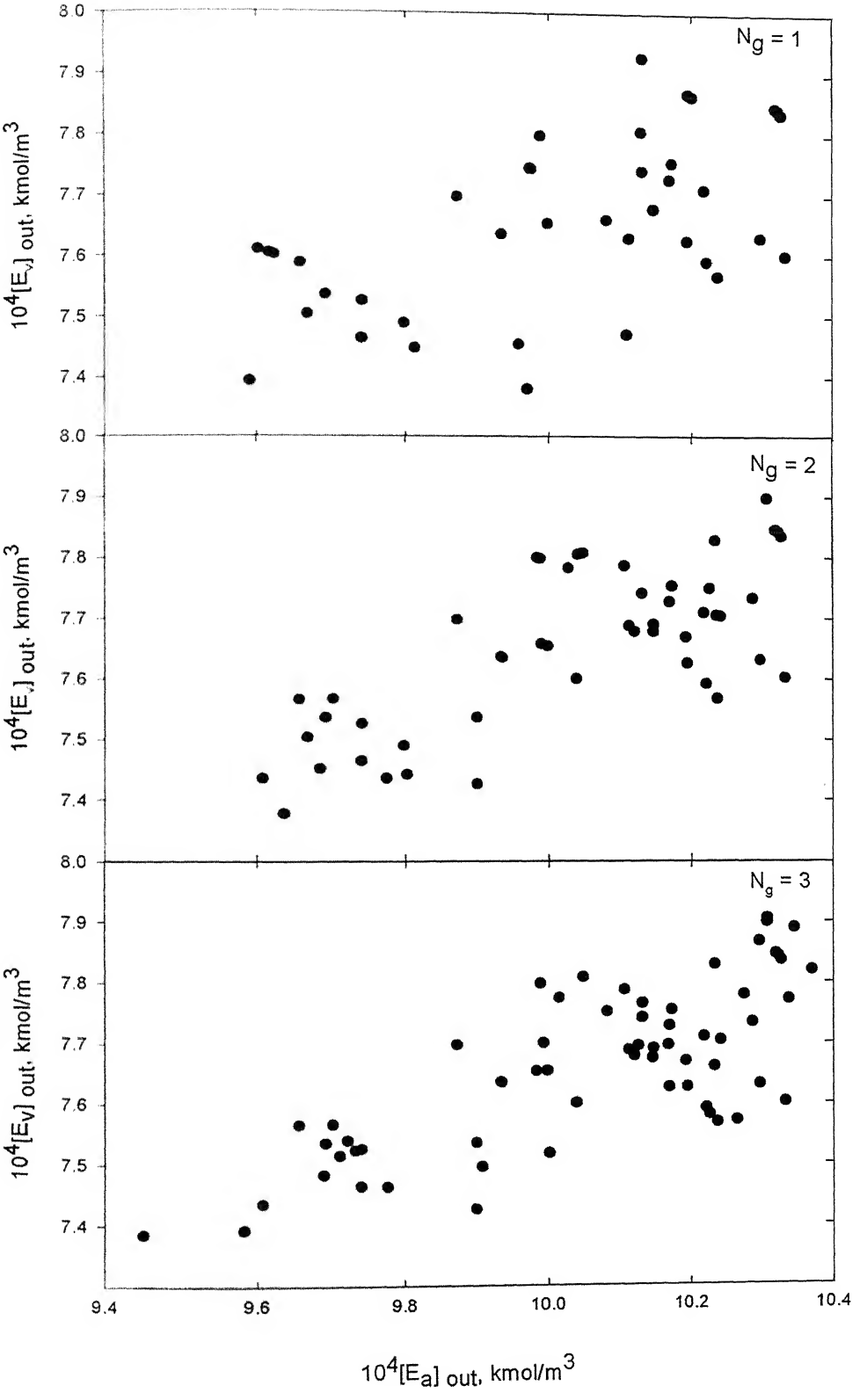

Fig. 4.1 $[E_a]_{out}$ *vs.* $[E_v]_{out}$ for the feasible chromosomes for different values of the generation number, N_g . The first three generations are shown. NSGA – II used.

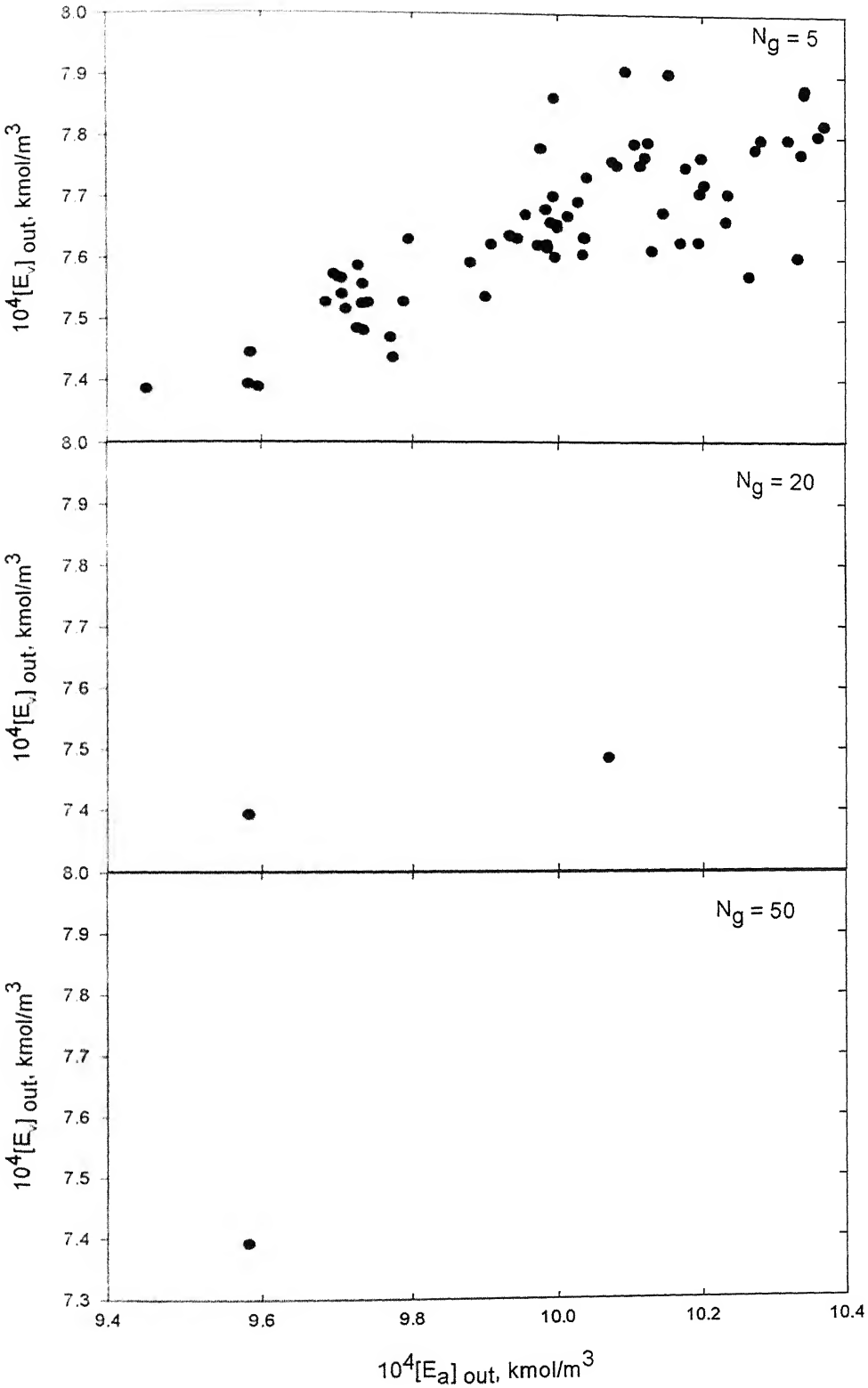

Fig. 4.2 $[E_a]_{out}$ vs. $[E_v]_{out}$ for the feasible chromosomes for Ng = 5, 20 and 50. NSGA – II used.

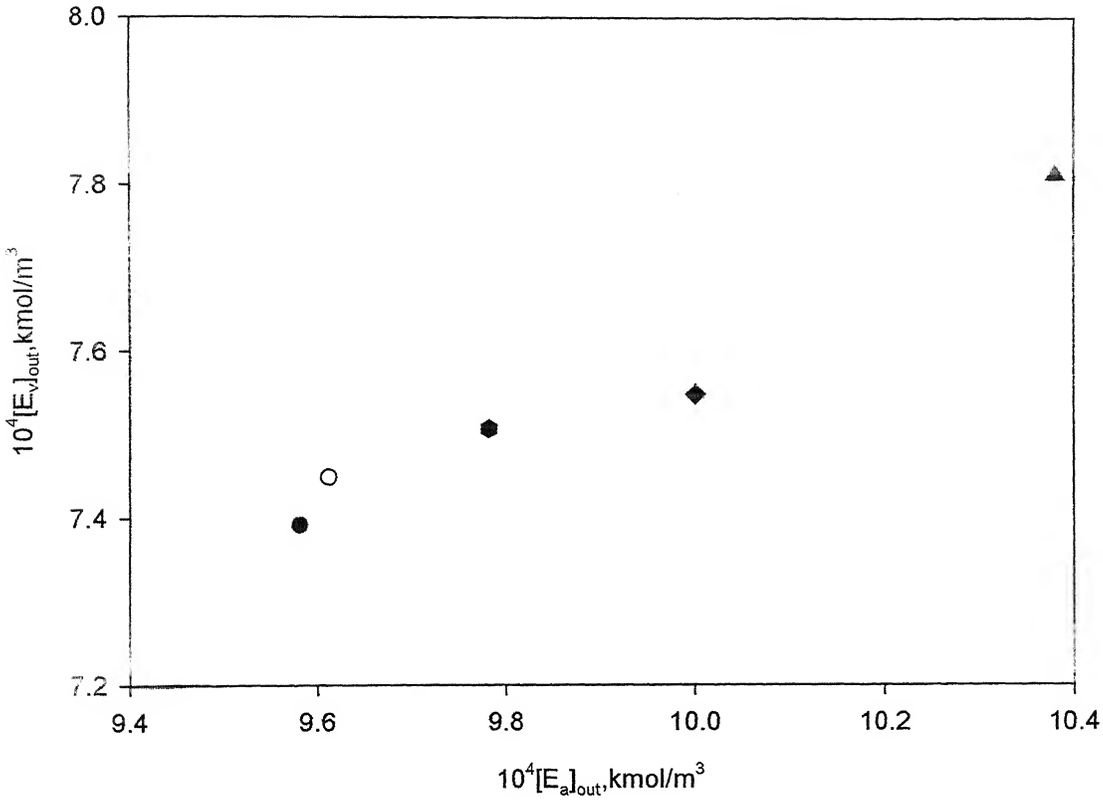

Fig. 4.3 $[E_a]_{out}$ vs. $[E_v]_{out}$ for the feasible chromosomes for N_g = 100. Filled circle - Optimal point obtained using NSGA – II. Filled Hexagon- Optimal point obtained using NSGA – I. Open circle - Optimal point obtained while minimizing I_1* and I_2* individually. Filled diamond represents optimal point as obtained by Bhaskar et al. (2000b). Filled triangle represents the present operating condition of the industrial wiped film reactor.

The multiobjective function optimization problem with end-point constraints has been solved using NSGA – I also. Figs. 4.4 and 4.5 show all the feasible solutions (i.e., those satisfying the end point constraints in Eqs. 4.1b-d) at different values of the generation number, N_g, when NSGA – I is used. For the same generation number, the chromosomes are found less scattered in the $[E_a]_{out}$ - $[E_v]_{out}$ space when NSGA – I is used. A unique optimal solution was obtained for this case, too (for Ng > 50). But NSGA – I converges to the unique optimal point in fewer generations than NSGA – II. Also, the concentrations of the acid and vinyl end groups in the product at the (unique) optimal point were higher than those obtained using NSGA – II. The solution is given by,

	NSGA – I	**NSGA - II**
$[E_a]_{out}$, kmol/m^3	9.78×10^{-4}	9.58×10^{-4}
$[E_v]_{out}$, kmol/m^3	7.5077×10^{-4}	7.392×10^{-4}
DP_{out}	82.000	82.000

The uniqueness of the optimal solution is checked out by performing an optimization using a single objective function. The objective functions, I_1* and I_2*, were taken, one at a time, and optimal solutions were generated under the same conditions as given in Eq. 4.1b-j (using NSGA – II). A unique optimal solution was obtained for this case also, but the values of the acid and vinyl end group concentrations were not the same as that obtained with the two objective function optimization problem. The optimal values of the acid and vinyl end group concentrations for the two cases are (using NSGA – II) :

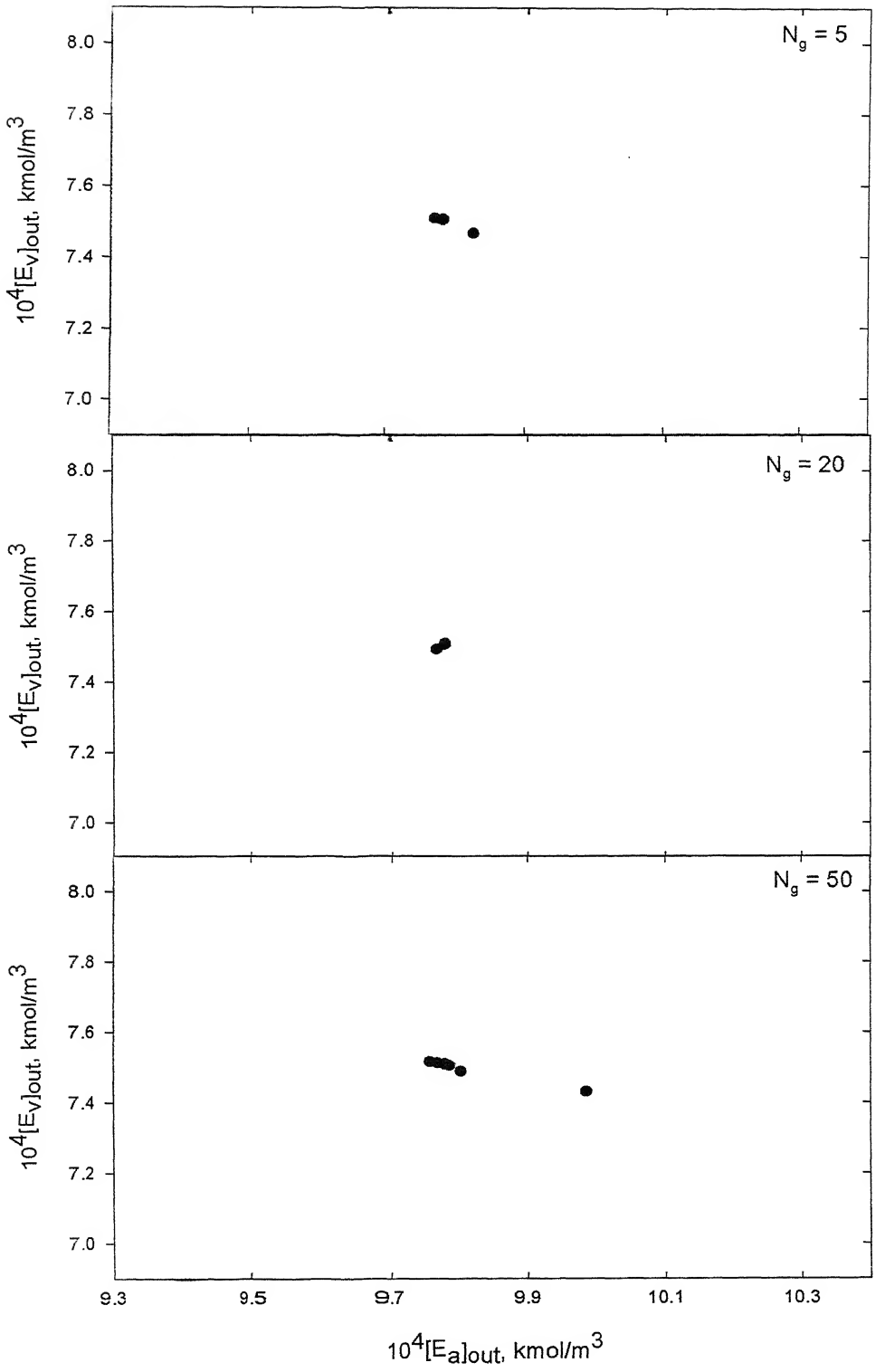

Fig. 4.5 $[E_a]_{out}$ vs. $[E_v]_{out}$ for the feasible chromosomes for Ng = 5, 20, 50. NSGA – I used.

	Min I_1*	Min I_2*
DP_{out}	82.00	82.00
$[E_a]_{out}$, kmol/m^3	9.61×10^{-4}	9.61×10^{-4}
$[E_v]_{out}$, kmol/m^3	7.45×10^{-4}	7.45×10^{-4}

This is in contrast to the study of Bhaskar et al. (2000b) who obtained a unique optimal solution when using a single objective function that is identical to that obtained for a two objective function optimization problem. This is quite interesting. It should be emphasized that GA (as well as NSGA) is an extremely robust technique [Goldberg (1989)] and should converge to the *global* optimal solution and also give *all* the optimal solutions where several exist. Clearly, this is not happening for either of the two algorithms.

Fig. 4.3 (N_g = 100) and Table 4.2 compare our optimal solutions obtained using NSGA – I and NSGA - II with the values corresponding to the current operation of the industrial wiped film reactor and that of Bhaskar et al. (2000b). It is observed that the optimal values of both the objective functions obtained with NSGA – II are, indeed, better than the present operating conditions of the industrial reactor. Lower values for both the acid and vinyl end group concentrations are obtained at a lower temperature. The lower temperature under optimal conditions lead to some energy savings.

The unique optimal solution was found to be affected significantly by the value of the seed number, Sr, used, in both NSGA – II and NSGA - I code (though unique points were *always* obtained, irrespective of the value of Sr). The results are shown in Fig. 4.6 for the six values of Sr given in Table 4.3. It is observed from Fig. 4.6a that both NSGA – II and NSGA – I converge to different (though unique) solutions, and both are unable to converge to the best solution in a

Table 4.3: Values of S_r used for the 5-decision variable problem

#	S_r
1 or a*	0.1298
2 or b	0.3219 (Ref. NSGA – II)
3 or c	0.3500
4 or d	0.6237 (Ref. NSGA – I)
5 or e	0.6755
6 or f	0.9740
7	0.8887 [Bhaskar et al (2000)]
8	Industrial

* 1,2,3,... Used for NSGA – II

a,b,c,... Used for NSGA - I

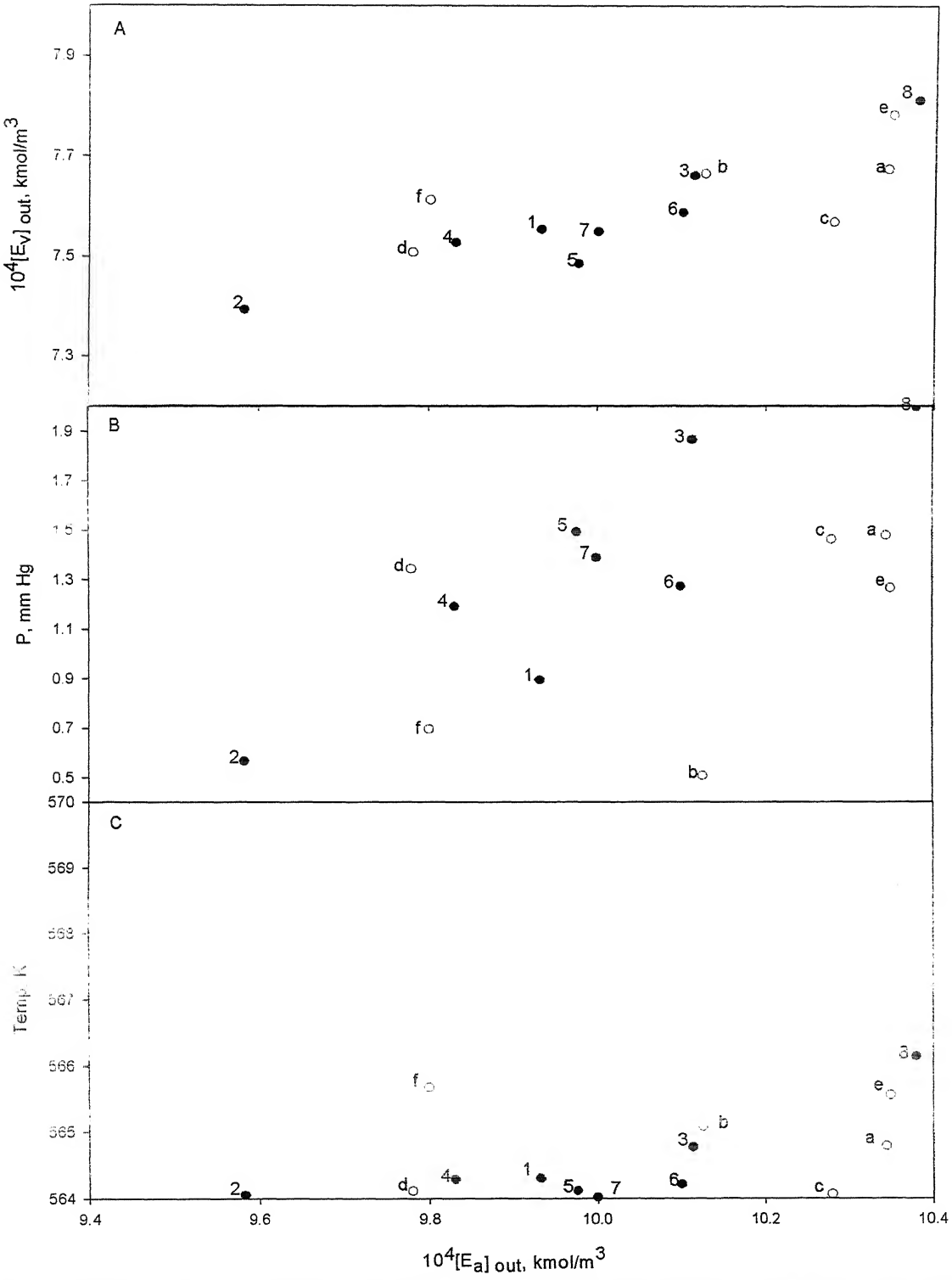

Fig. 4.6 Optimum results for several values of Sr (see Table 4.3) for Eq. 4.1 (Figure A). Values of the decision variables, P and T, for the optimal points are shown in Figs. B, C. (• - NSGA – II , o – NSGA – I).

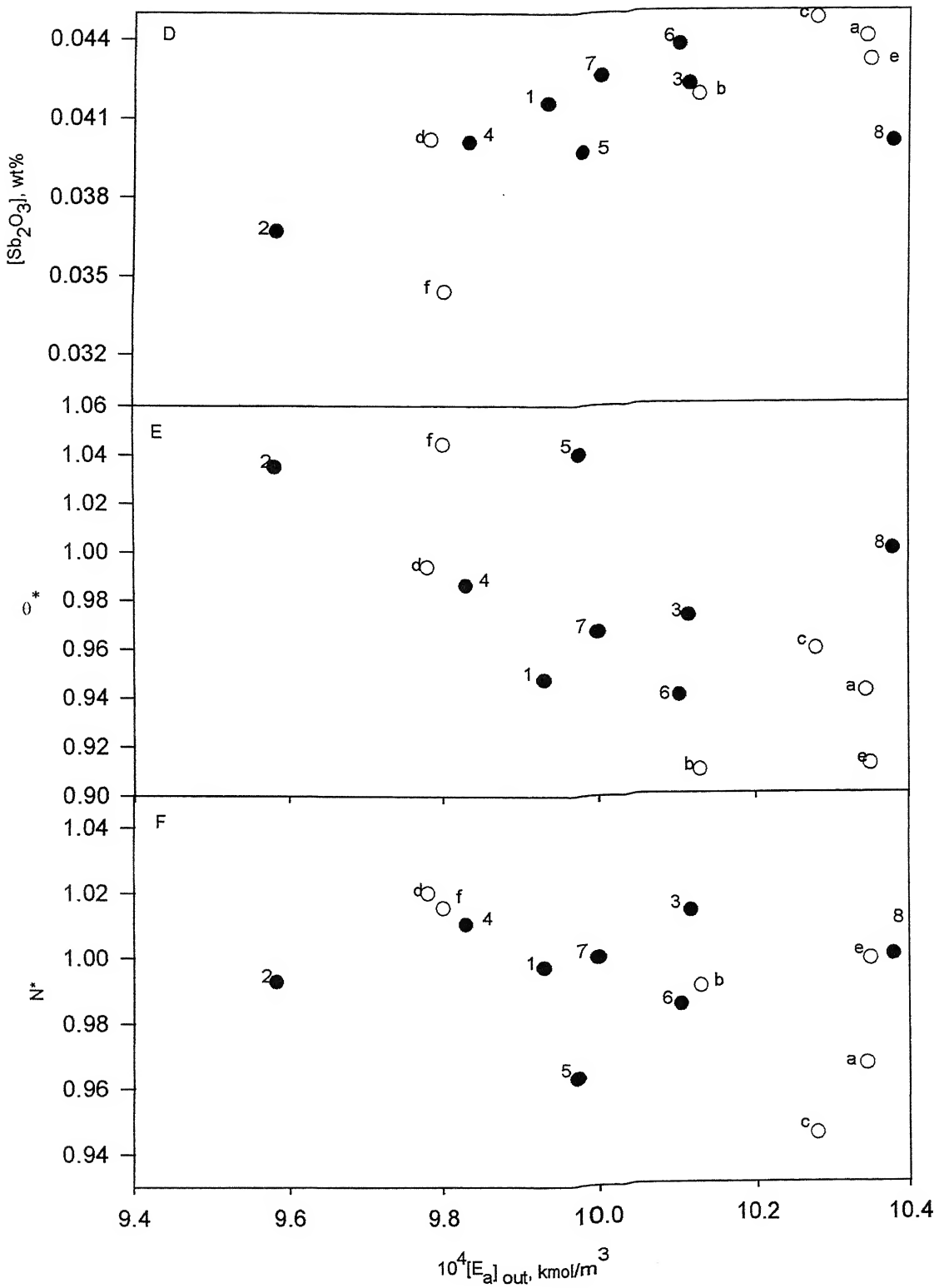

Fig. 4.6 (Contd...) Values of the decision variables [Sb_2O_3], θ* and N*, for the optimal points for several values of Sr (see Table 4.3). (• - NSGA – II , o – NSGA – I).

single application. The sensitivity of NSGA to one of the computational parameters may be a manifestation of premature convergence. This has been alluded to by Goldberg (1989) himself, who mentioned that even though GAs are quite efficient in reaching the global-optimum *region*, they are not guaranteed to reach the *precise location* of the global-optimum *point(s)*, particularly for complex problems, and may converge prematurely.

Another interesting point suggested by Figure 4.6 is that even for near-identical values of the two objective functions, as for example, points 1 and 5 (for NSGA – II) corresponding to values of S_r of 0.1298 and 0.6755, and points a and e (for NSGA – I) corresponding to values of S_r of 0.1298 and 0.6755, the decision variables differ significantly. We refer to this as the problem of sensitivity of optimal solutions.

The effect of the weightage factor, w_2, was studied in detail (using both NSGA – II and NSGA - I). Fig. 4.7 shows the results for six sets of values of Sr (as given in Table 4.3, except for Sr = 0.3219 and Sr = 0.6755 for NSGA – II and Sr = 0.6237 for NSGA – I), when w_2 is taken as 10^4 (instead of 10^8). Different (though unique) optimal points are obtained, but the optimal value of the acid and vinyl end group concentrations obtained for each of these Sr is lower (better) than those obtained with $w_2 = 10^8$. Thus, our earlier conjecture that premature convergence is associated with the use of inappropriate GA parameters, is confirmed. The problem of sensitivity was not observed in this case. The use of a lower value of w_2, however, does not give rise to *unique* solutions when Sr = 0.3219 and Sr = 0.6755 for NSGA – II and Sr = 0.6237 for NSGA – I. In these cases, deviations of DP_{out} from DP_d (of $\pm$ 0.15 for $w_2 = 10^4$) are observed. These points are not included in Fig. 4.7. Figs. 4.8, 4.9 and 4.10 show values of $[E_a]_{out}$ *vs.* $[E_v]_{out}$ and the corresponding values of the decision variables (P,T,$[Sb_2O_3]$, N*, θ*) *vs.* $[E_a]_{out}$ for these three cases.

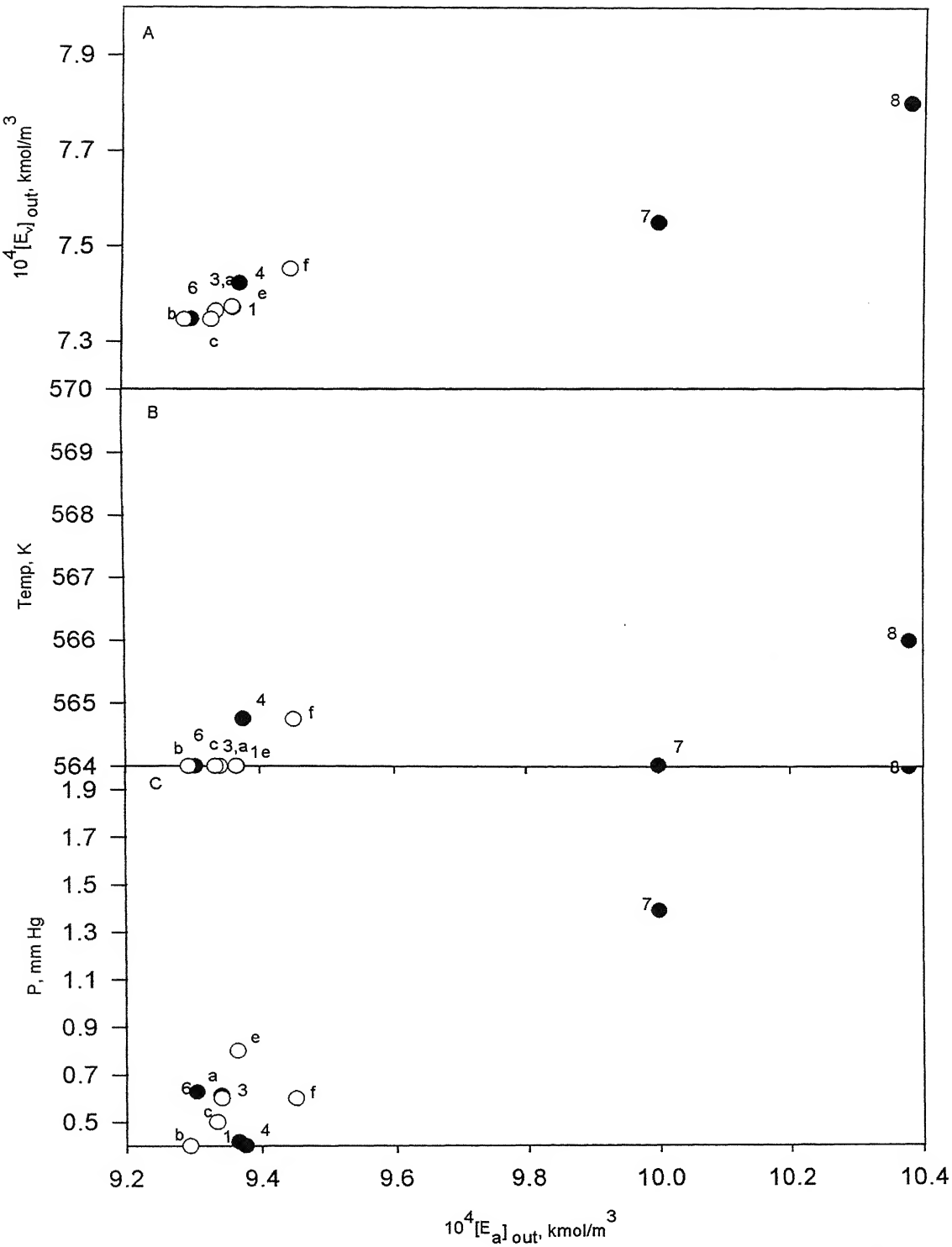

Fig. 4.7 Optimum solutions for several values of Sr (Table 4.3) for Eq. 4.1. The value of the weightage factor, w_2, is 10^4. Point b represents the global optimum solution. Values of the decision variables, P and T, for the optimal points are shown in Figs. B, C. (• - NSGA – II, o – NSGA – I)

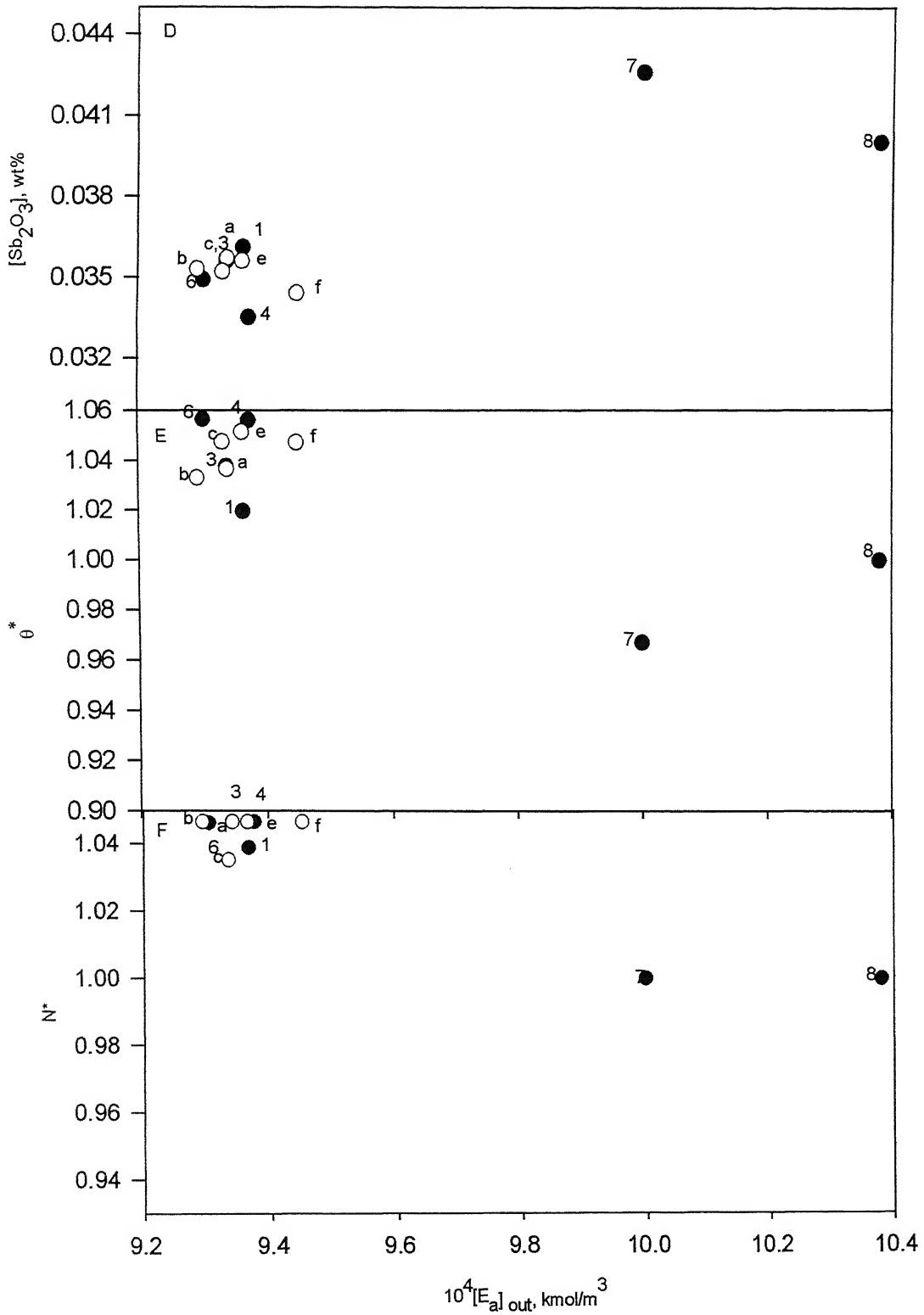

Fig. 4.7 (Contd...) Values of the decision variables, $[Sb_2O_3]$, θ* and N*, for optimal points for several values of Sr (see Table 4.3) . (• - NSGA – II , o – NSGA – I).

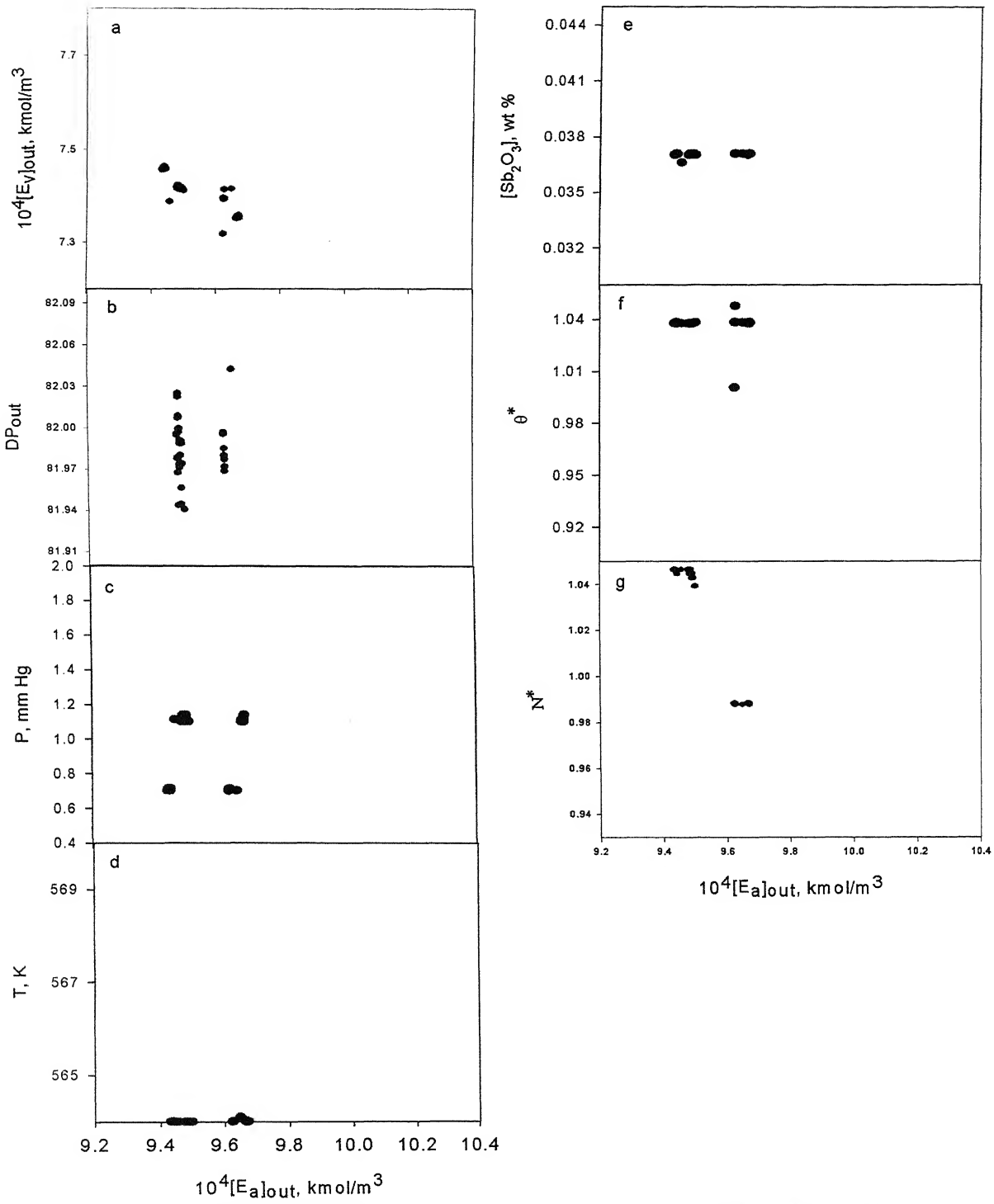

Fig. 4.8 Optimum values of $[E_a]_{out}$ *vs.* $[E_v]_{out}$ obtained using NSGA – II for Sr = 0.3219 for the five decision variable problem of Eq. 4.1 (Figure a). $w_2 = 1 \times 10^4$. c-g represent the corresponding values of the decision variables (P,T,$[Sb_2O_3]$, N*, θ*). Unique optimal solution is not obtained in this case.

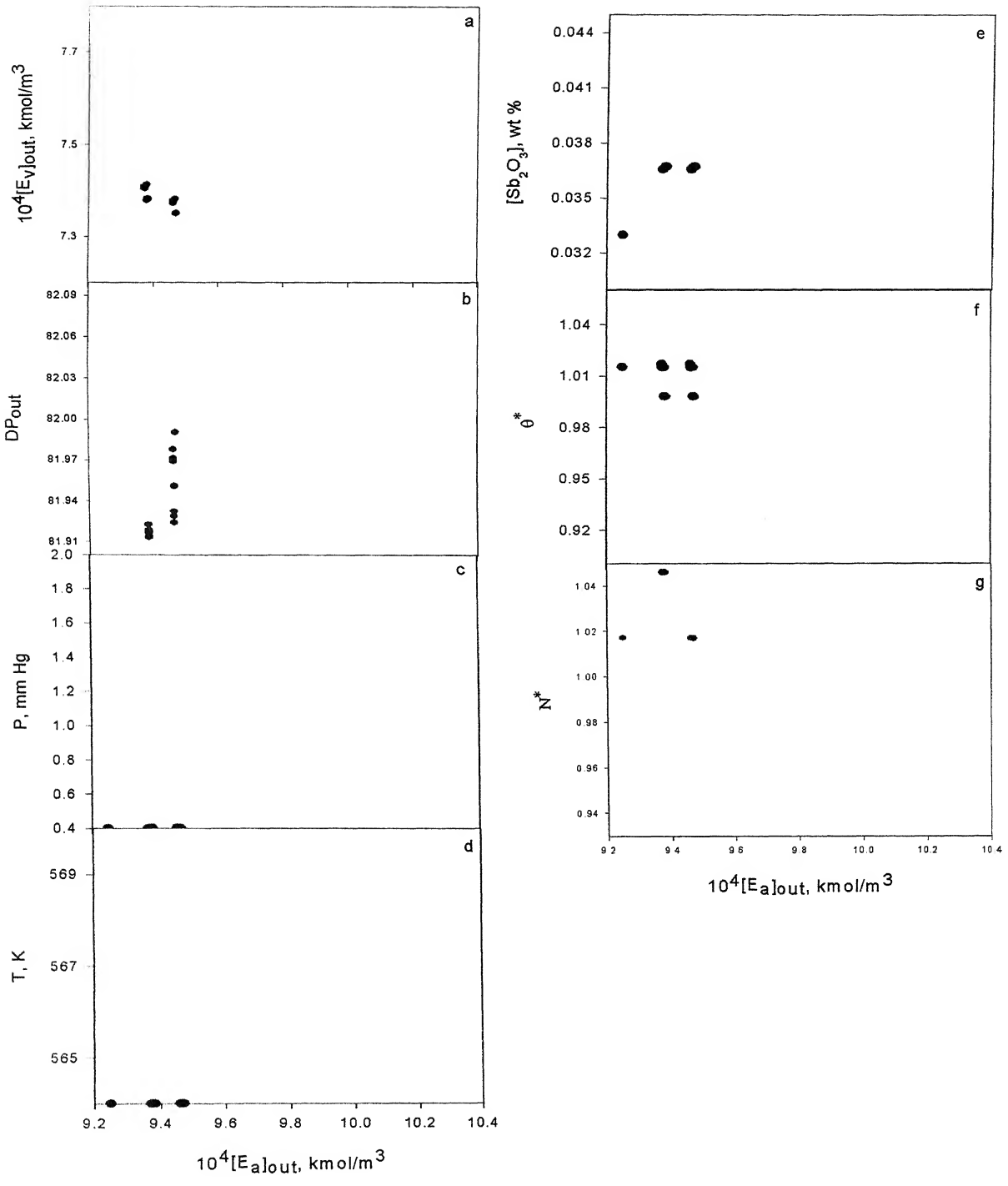

Fig. 4.9 Optimum values of $[E_a]_{out}$ *vs.* $[E_v]_{out}$ obtained using NSGA – II for Sr = 0.6755 for the five decision variable problem of Eq. 4.1 (Figure a). $w_2 = 1 \times 10^4$. c-g represent the corresponding values of the decision variables (P,T,$[Sb_2O_3]$, N*, θ*). Unique optimal solution is not obtained in this case.

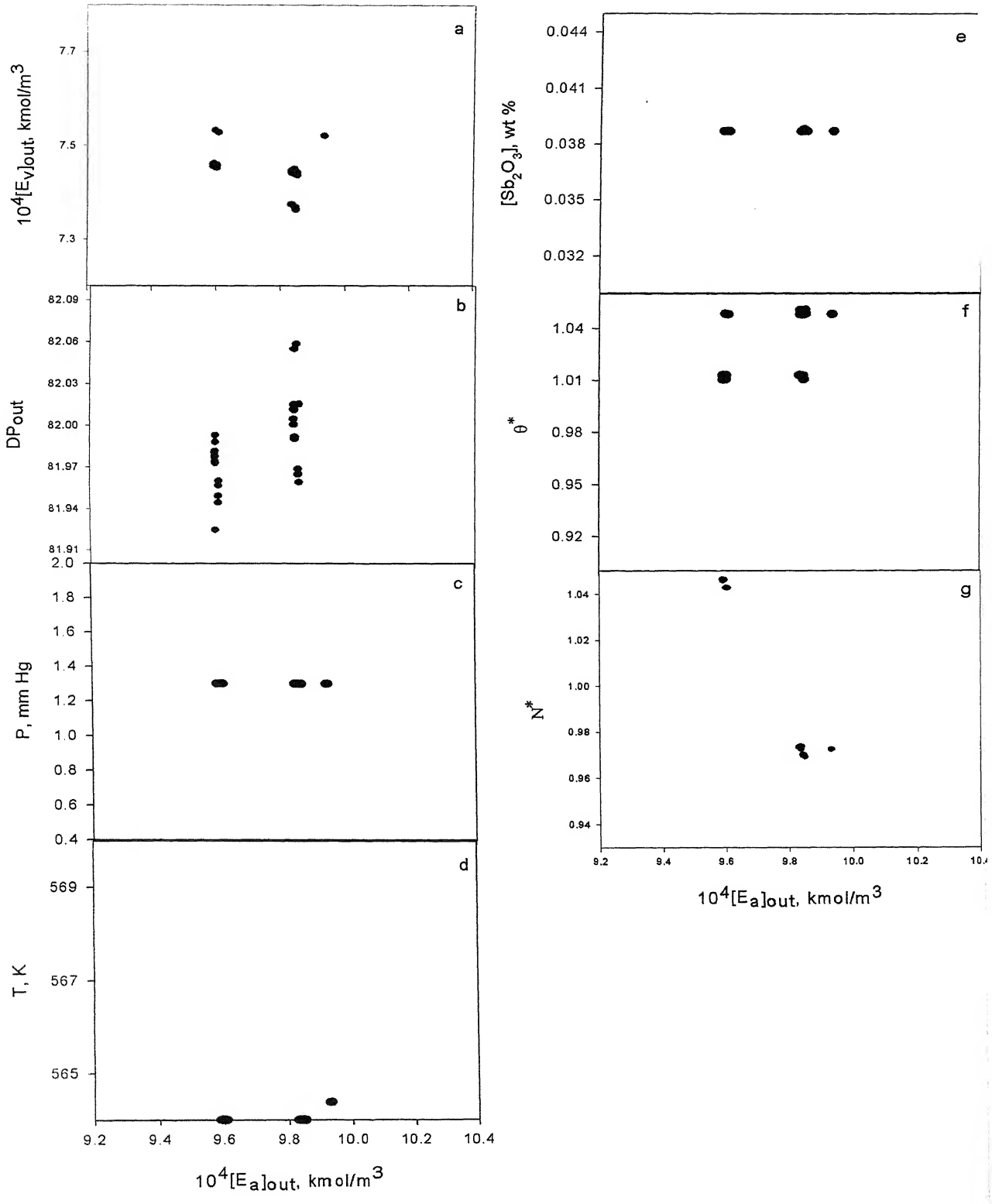

Fig. 4.10 Optimum values of $[E_a]_{out}$ *vs.* $[E_v]_{out}$ obtained using NSGA – I for Sr = 0.6237 for the five decision variable problem of Eq. 4.1 (Figure a). $w_2 = 1 \times 10^4$. c-g represent the corresponding values of the decision variables (P,T,$[Sb_2O_3]$, N*, θ*). Unique optimal solution is not obtained in this case.

We modified the problem in Eq. 4.1 to one involving only four decision variables, and kept the temperature at a constant value of 564.0 K. The results obtained using NSGA – I and NSGA – II (using $w_2 = 1\times10^4$) for the six sets of values of Sr (Table 4.3) are shown in Fig. 4.11. Different (though unique) local optimal points were obtained for this problem *also* and these points do not form a Pareto set, unlike what was observed by Bhaskar et al. (2000c). Similar to what was observed previously, lower values of w_2, do not give rise to *unique* solutions when Sr = 0.3219 and Sr = 0.3500 for NSGA – II and Sr = 0.3219, 0.3500 and 0.6237 for NSGA – I. In these cases deviations of DP_{out} from DP_d (of $\pm$ 0.15 for $w_2 = 10^4$) are observed. These points are not included in Fig. 4.11. Values of $[E_a]_{out}$ *vs.* $[E_v]_{out}$ and the corresponding values of the decision variables (P,T,$[Sb_2O_3]$, N*, θ*) *vs.* $[E_a]_{out}$ for these cases are shown in Figs. 4.12 - 4.16.

4.4 Summary

An improved re–tuned model for the finishing reactor in PET manufacture is developed. Minimization of the degradation side products, $[E_a]_{out}$ and $[E_v]_{out}$, was carried out using NSGA – I and NSGA - II. P, T, $[Sb_2O_3]$, θ* and N* were used as the decision variables. An end-point constraint was imposed on DP_{out}, while the concentration, $[E_a]_{out}$, was constrained to lie below a maximum value. In addition, an allowable range was prescribed for $[E_{DEG}]_{out}$. A unique solution was obtained for this multiobjective optimization problem. No Pareto set of non-inferior solutions was obtained. Problems of sensitivity and premature convergence were encountered when different values of Sr (randomseed numbers) are used to obtain the optimal solutions. When w_2 is reduced from 10^8 to 10^4, problems of sensitivity and premature convergence were not encountered, and optimal values of both the objective functions obtained using NSGA – I and

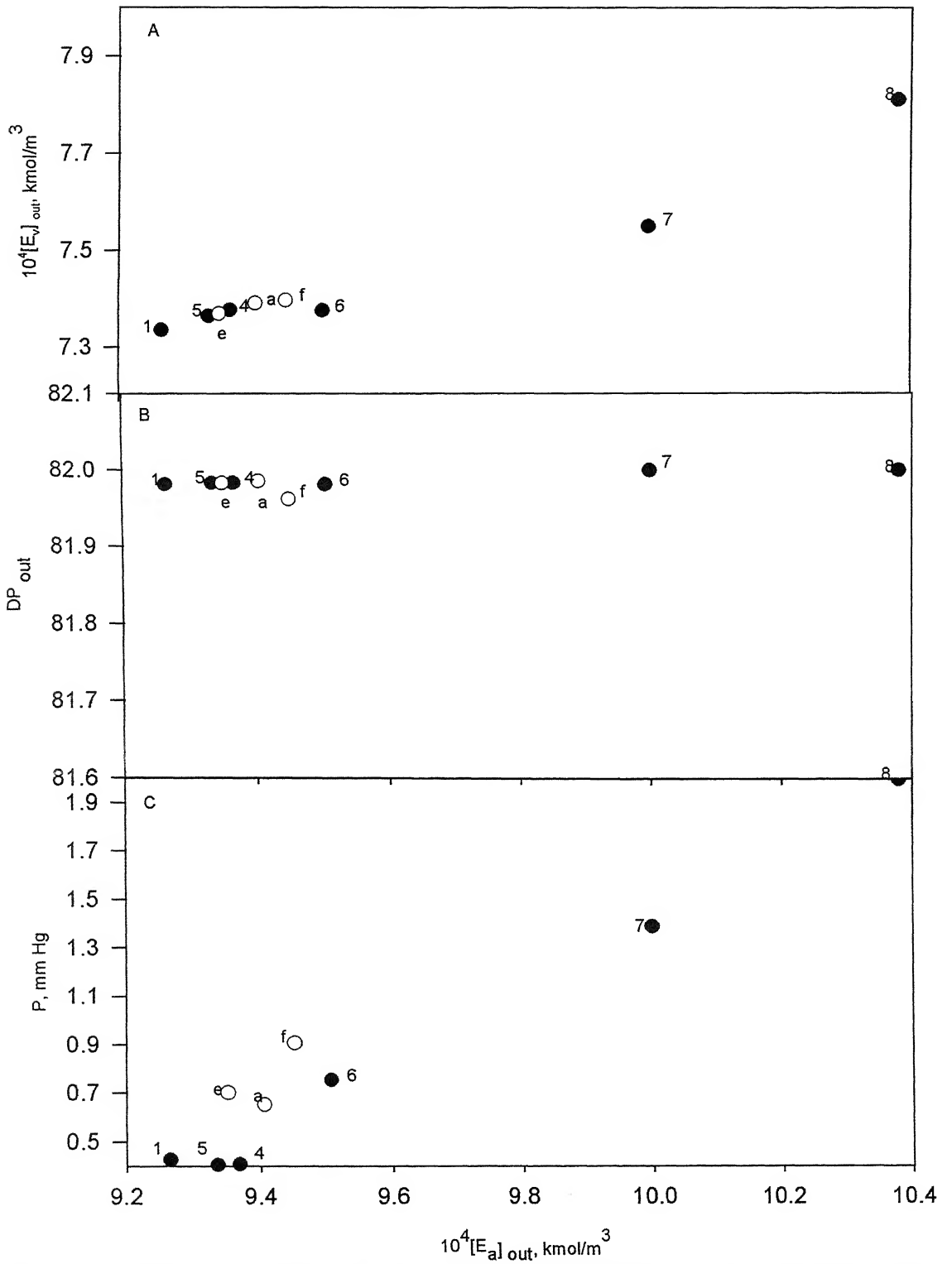

Fig. 4.11 Optimum solutions for several values of Sr (Table 4.3) for the four decision variable problem at T = 564.00 K. $w_2 = 10^4$. (• - NSGA – II, o – NSGA – I).

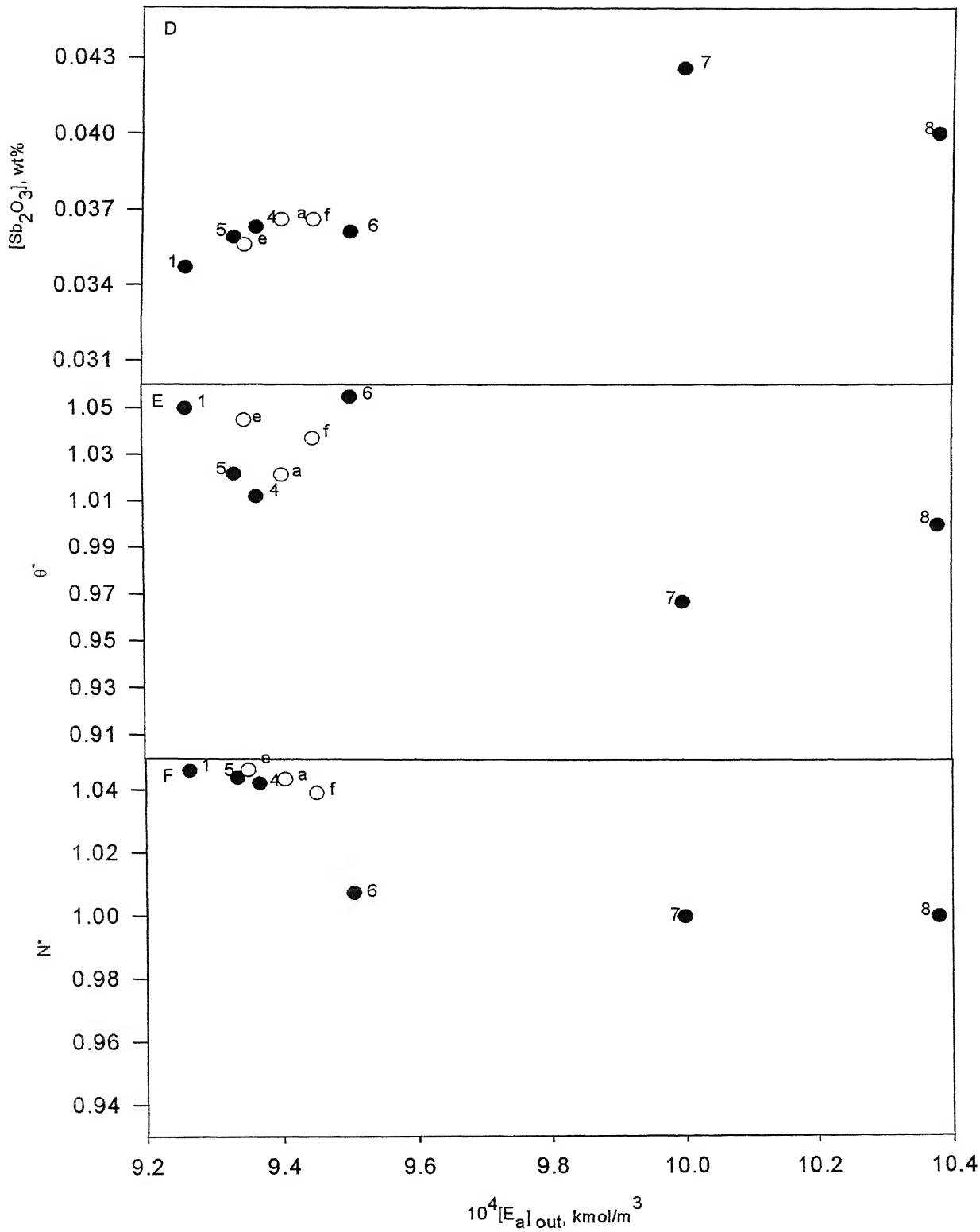

Fig. 4.11 (Contd...) Values of the decision variables, $[Sb_2O_3]$, θ* and N* for the optimal points in Fig. 4.11a for several values of Sr (see Table 4.3) . (• - NSGA – II , o – NSGA – I).

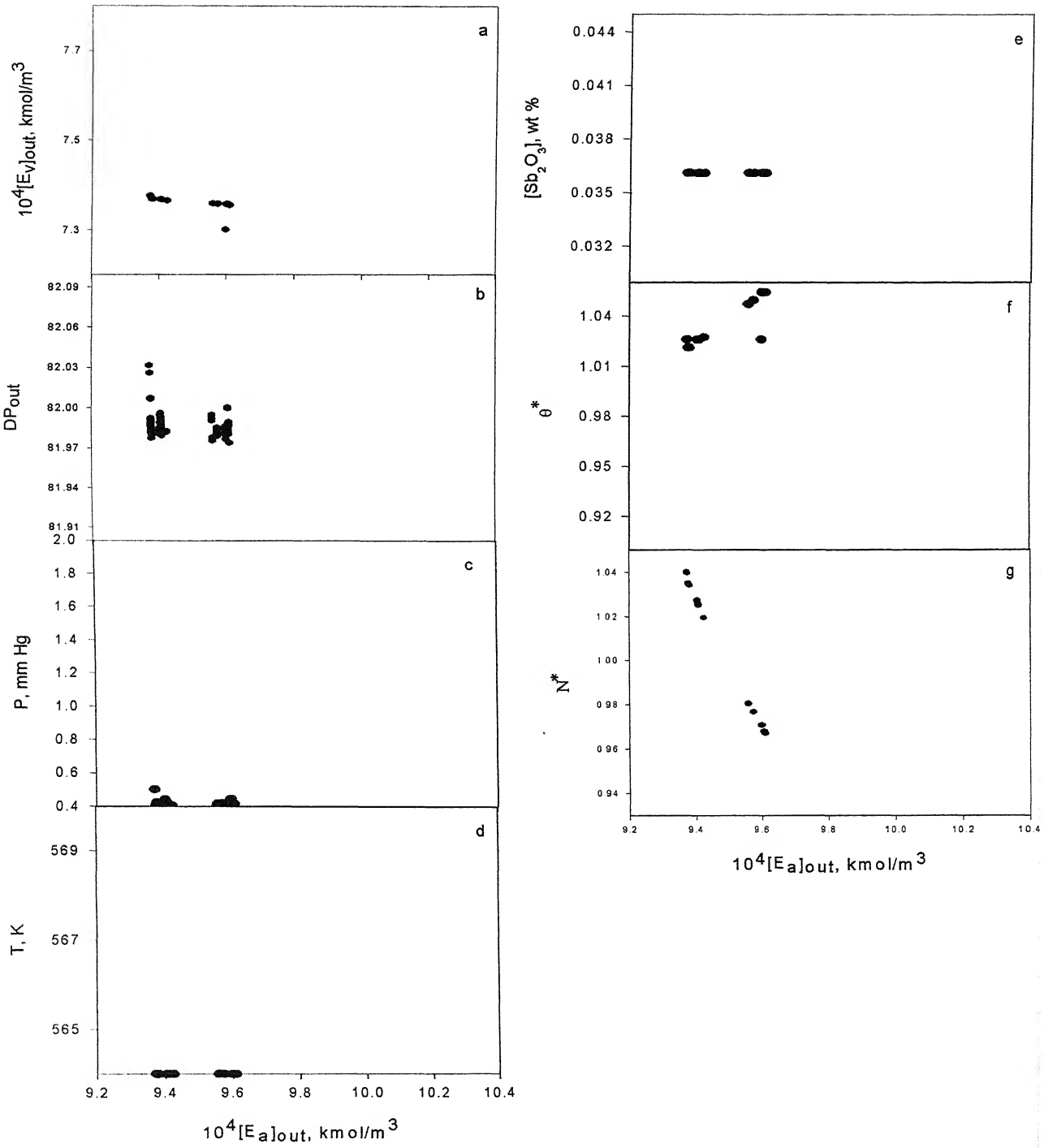

Fig. 4.12 Optimum values of $[E_a]_{out}$ *vs.* $[E_v]_{out}$ obtained using NSGA – II for Sr = 0.3219 for the four decision variable problem at T = 564.00 K (Figure a). $w_2 = 1 \times 10^4$. c-g represent the corresponding values of the decision variables (P,T,$[Sb_2O_3]$, N*, θ*). Unique optimal solution is not obtained in this case.

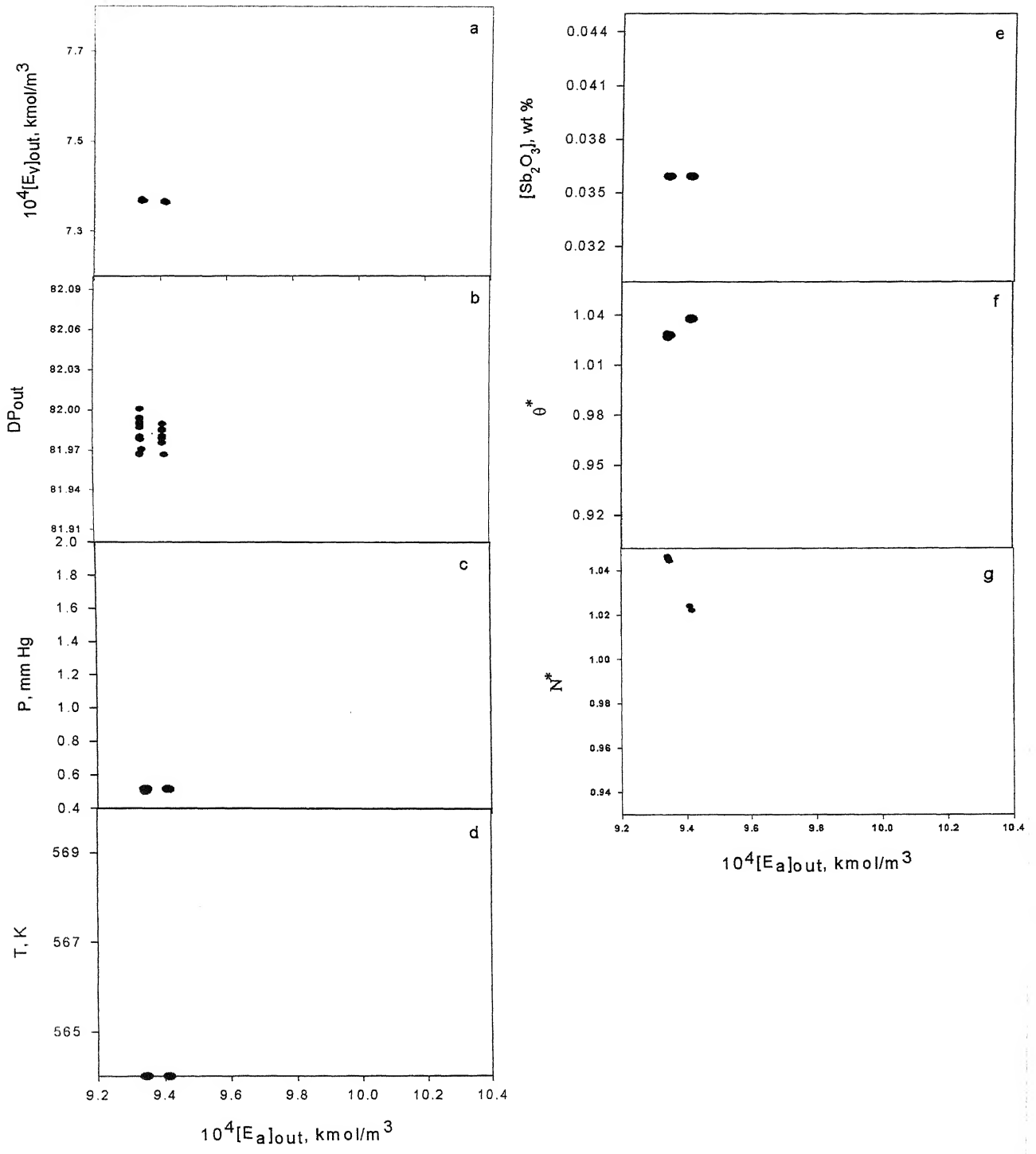

Fig. 4.13 Optimum values of $[E_a]_{out}$ *vs.* $[E_v]_{out}$ obtained using NSGA – II for Sr = 0.3500 for the four decision variable problem at T = 564.00 K (Figure a). $w_2 = 1 \times 10^4$. c-g represent the corresponding values of the decision variables (P,T,$[Sb_2O_3]$, N*, θ*). Unique optimal solution is not obtained in this case.

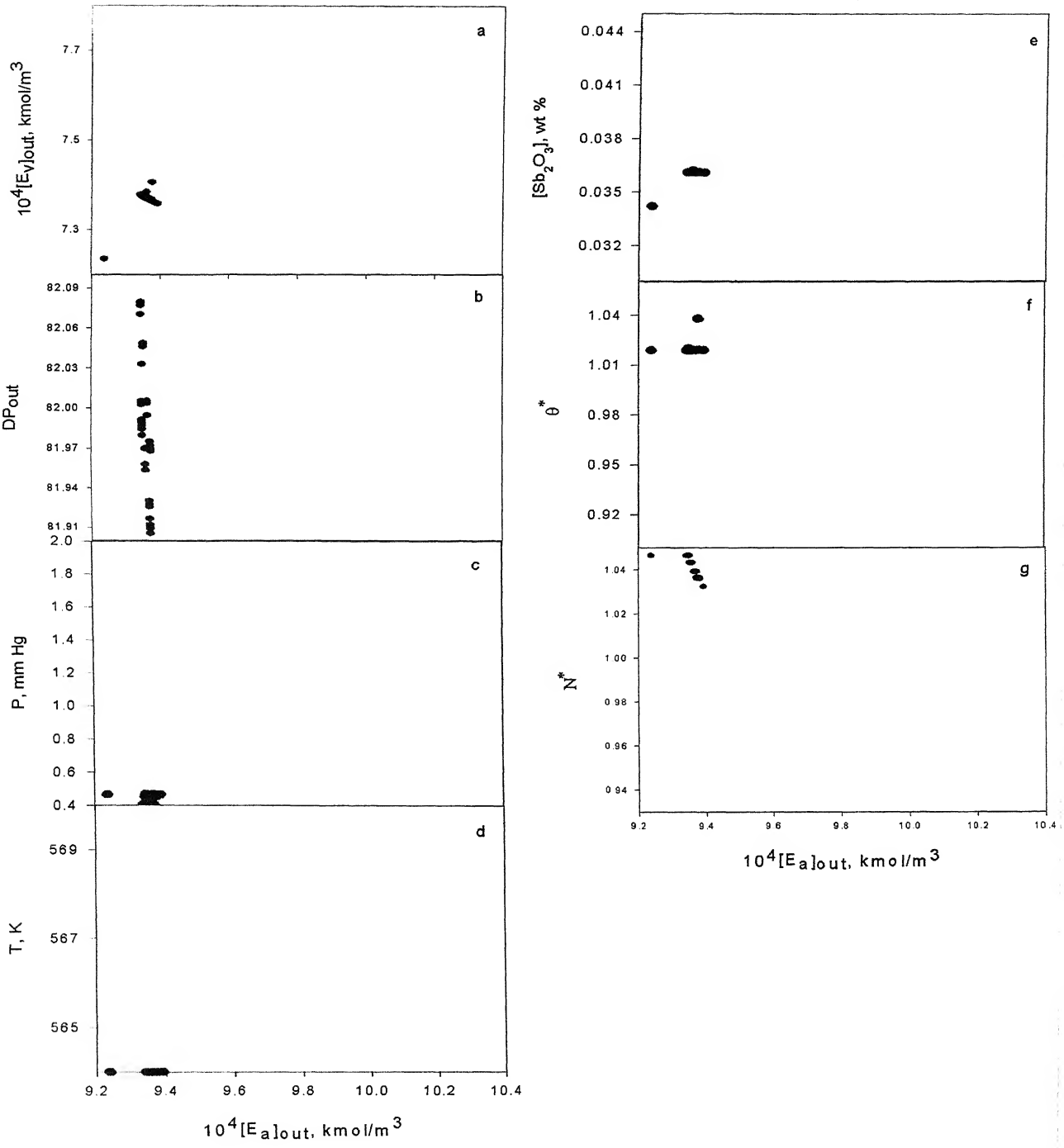

Fig. 4.14 Optimum values of $[E_a]_{out}$ *vs.* $[E_v]_{out}$ obtained using NSGA – I for Sr = 0.3219 for the four decision variable problem at T = 564.00 K (Figure a). $w_2 = 1 \times 10^4$. c-g represent the corresponding values of the decision variables (P,T,$[Sb_2O_3]$, N*, θ*). Unique optimal solution is not obtained in this case.

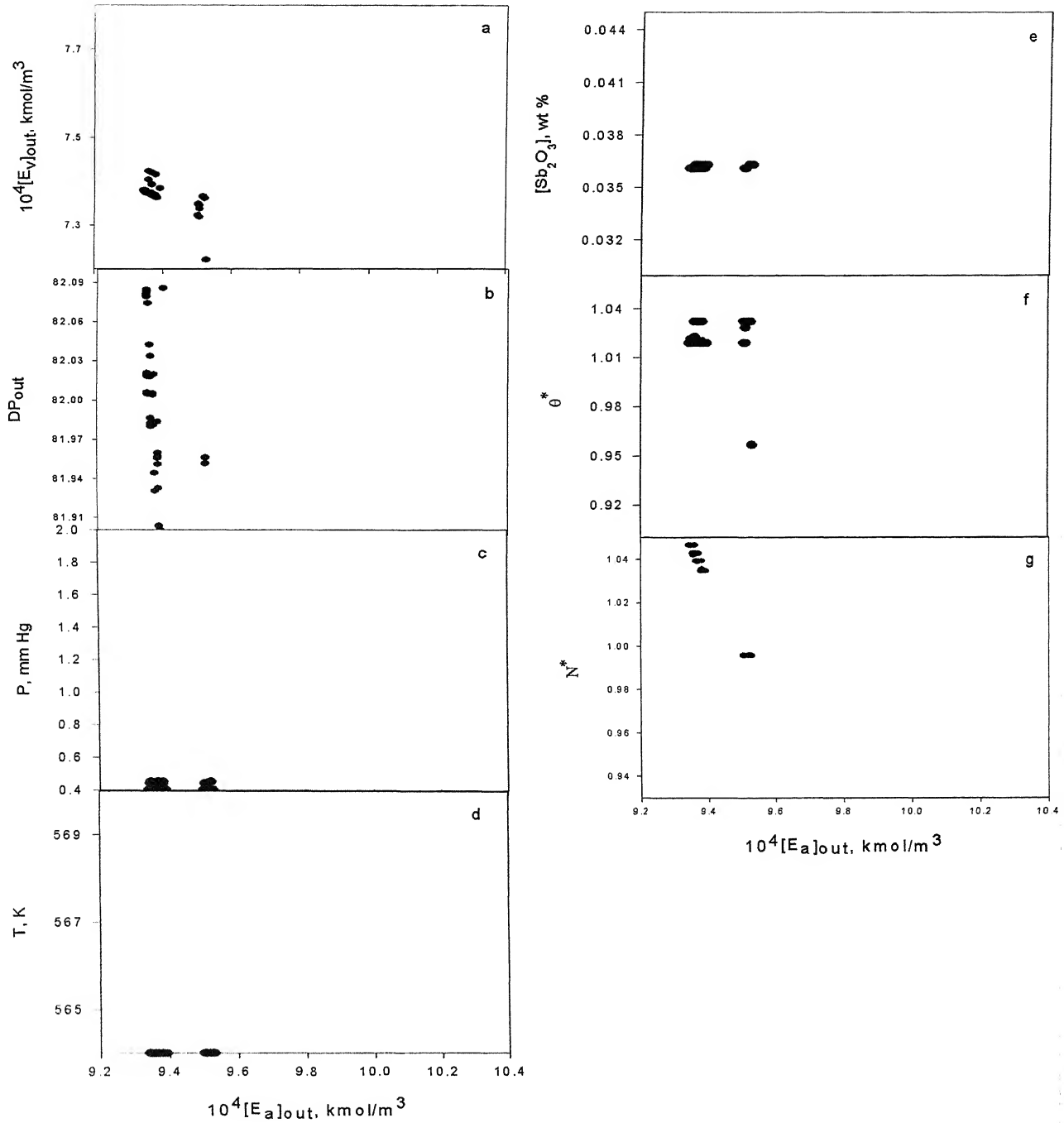

Fig. 4.15 Optimum values of $[E_a]_{out}$ *vs.* $[E_v]_{out}$ obtained using NSGA – I for Sr = 0.3500 for the four decision variable problem at T = 564.00 K (Figure a). $w_2 = 1 \times 10^4$. c-g represent the corresponding values of the decision variables (P,T,$[Sb_2O_3]$, N*, θ*). Unique optimal solution is not obtained in this case.

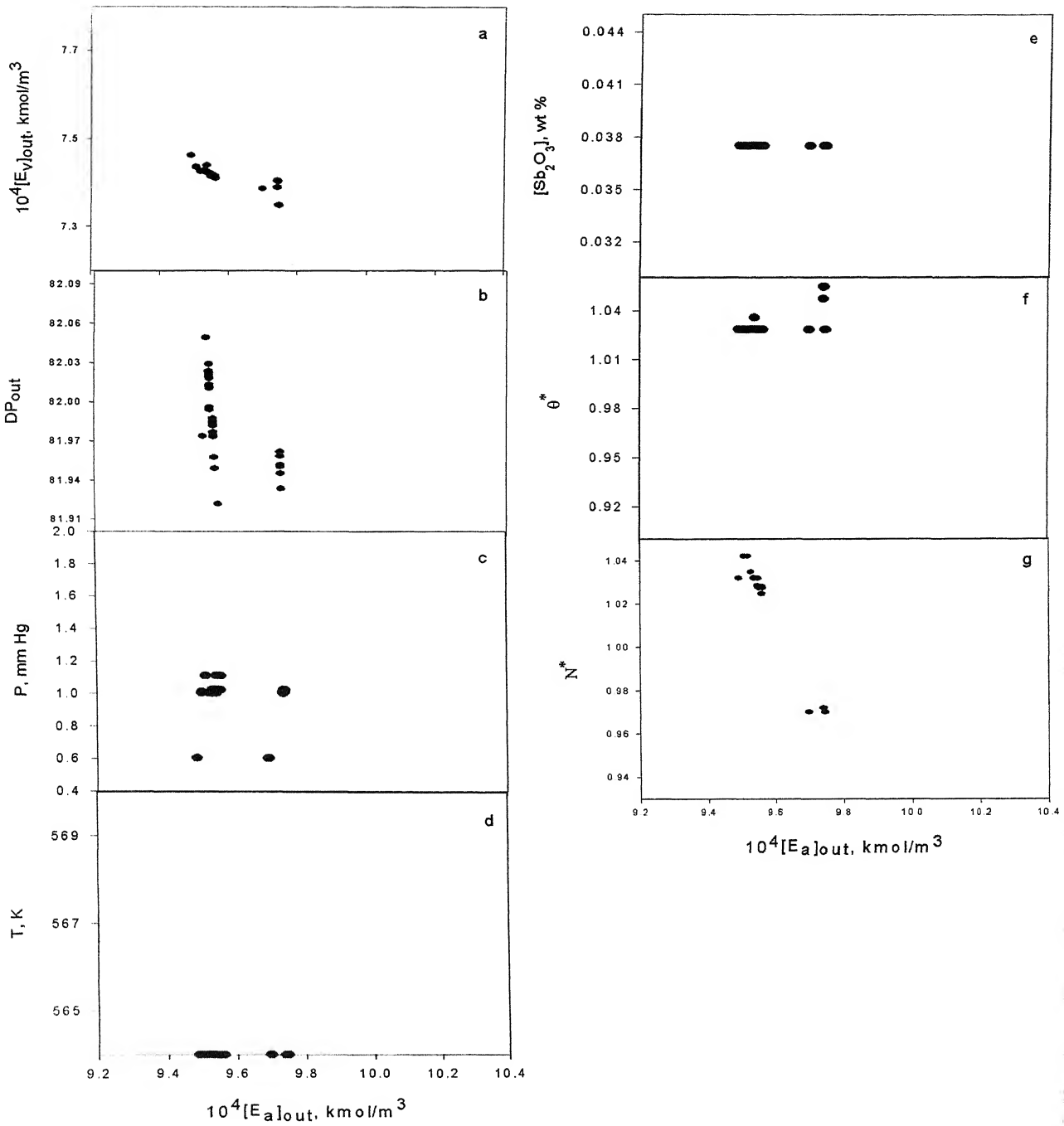

Fig. 4.16 Optimum values of $[E_a]_{out}$ *vs.* $[E_v]_{out}$ obtained using NSGA – I for Sr = 0.6237 for the four decision variable problem at T = 564.00 K (Figure a). $w_2 = 1 \times 10^4$. c-g represent the corresponding values of the decision variables (P,T,$[Sb_2O_3]$, N*, θ*). Unique optimal solution is not obtained in this case.

NSGA – II are almost identical even with the use of different values of Sr. However, in some cases due to deviation of DP_{out} from DP_d, unique optimal points are not obtained. Unique optimal points were obtained even when the temperature is kept constant and *not* used as a decision variable (except in some cases, where deviation of DP_{out} from DP_d value is observed), in contrast to the study of Bhaskar et al. (2000c).

Chapter 5 : CONCLUSIONS AND SUGGESTIONS FOR FUTURE WORK

The model of Bhaskar et al. (2000a) has been modified and re–retuned to describe industrial data for a wiped film PET reactor. Industrial data involving commercially important product properties like DP_{out} and the concentrations of the DEG and acid end groups in the product, have been used. The parameters tuned are k_La_{ref}, the Flory-Huggins' interaction parameter, χ_1, the equilibrium constants, K_1, K_5 and K_8, the frequency factors of three-rate constants, k_2, k_3 and k_9, and α, a parameter associated with the effect of the RPM of the agitator on k_La. These parameters are tuned using three sets of industrial data. The tuned parameters are then used unchanged to predict the concentration of the various side products and the DP_{out} for a different operating temperature. It is found that the model predicts these values very well.

Minimization of the degradation side products, $[E_a]_{out}$ and $[E_v]_{out}$, was carried out using NSGA – I and NSGA – II. P, T, $[Sb_2O_3]$, θ^* and N^* were used as the decision variables. An end-point constraint was imposed on DP_{out}, while the concentration, $[E_a]_{out}$, was constrained to lie below a maximum value. In addition, an allowable range was prescribed for $[E_{DEG}]_{out}$. Unique solutions were obtained for this multiobjective optimization problem using both algorithms. No Pareto set of non-inferior solutions was obtained. Problems of sensitivity, premature convergence and scatter were encountered when both NSGA – I and NSGA – II were used for solving this problem.

5.1 Future Work

The following are some of the challenging areas to attempt to understand the PET reactor systems:

- Kinetic model for PET reactor systems could further be explored to have reliable and accurate kinetic data.
- More work could be done to understand the effect of the Flory-Huggins' interaction parameter (χ_1) and the mass-transfer parameter (k_La) on the polymer formation of PET.

REFERENCES

Amon, M. and C. D. Denson. Simplified Analysis of the Performance of Wiped-Film Polycondensation Reactors. *Ind. Eng. Chem. Fundam.*, **19**, 415, 1980.

Barkley, K. T. and W. L. Predmore. Process for Removing Metallic Antimony from Polyester Prepolymers. U. S. Patent 3,497,477, Feb 24, 1970.

Besnoin, J. M., and K.Y.Choi. Identification and Characterization of Reaction Byproducts in the Polymerization of Polyethylene Terephthalate. *J. Macromol. Sci., Rev. Macromol. Chem. Phys.*, **C29**, 55, 1989.

Beveridge, G. S. G. and R.S. Schechter. Optimization: Theory and Practice. New York: McGraw Hill, 1970.

Bryson, A. E. and Y. C. Ho. Applied Optimal Control. Waltham: Blaisdell, 1969.

Bhaskar, V., S. K. Gupta, and A. K. Ray. Modeling of an Industrial Wiped Film Poly (ethylene terephthalate) reactor, *Polym. Reac. Eng.*, **8**,000 , 2000a.

Bhaskar, V., S. K. Gupta, and A. K. Ray. Multiobjective optimization of an Industrial Wiped Film PET reactor, *AIChE J.*, **46(5)**, 1046 , 2000b.

Bhaskar, V., S. K. Gupta, and A. K. Ray. Multiobjective optimization of an Industrial Wiped Film poly (ethylene terephthalate) reactor: some further insights, *Computers and Chemical Engineering*, **25**, 391, 2001.

Bhaskar, V., S. K. Gupta, and A. K. Ray. Applications of Multiobjective Optimization in Chemical Engineering, *Revs. Chem. Eng.*, **16(1)**, 1, 2000c.

Chan, C.Y., Aatmeeyata, S. K. Gupta, and A. K. Ray. Multiobjective Optimization of Membrane Separation Modules, *J. Memb. Sci.*, **176,** 2000.

Chankong, V., and Y. Y. Haimes. Multiobjective Decision Making – Theory and Methodology. New York: Elsevier. 1983.

Cheong, S. I. and K. Y. Choi. Melt Polycondensation of Poly(Ethylene-Terephthalate) in a Rotating-Disk Reactor. *J. Appl. Polym. Sci.,* **58**, 1473, 1995.

Cheong, S. I. and K. Y. Choi. Modeling of a Continuous Rotating Disk Polycondensation Reactor for the Synthesis of Thermoplastic Polyesters. *J. Appl. Polym. Sci.,* **61**, 763. 1996.

Chimaru, K. Ito, S. Takashima, Y. Yoshihiro and M. Shindo. Process for Preparing Linear Polyesters. U.S. Patent, 3,732,182, May 8, 1973.

David, E. J. and G. P. Lawrence. Effect of Reaction Time on Poly(ethylene Terephthalate) Properties. *Ind.Eng.Chem.Res.,* **34**, 4049, 1995.

Deb, K.. Genetic Algorithms in Multimodel function Optimization (TCGA Report No. 89002) Tuscaloosa, AL: University of Alabama, The Clearing House For Genetic Algorithms. 1989.

Deb, K.. Optimization for Engineering Design: Algorithms and Examples, Prentice Hall of India, New Delhi, 1995.

Deb K., Amrit Pratap, Sameer Agarwal and T. Meyarivan. A Fast and Elitist Multi-Objective Genetic Algorithm-NSGA-II. *KanGAL Report Number 2000001*, IIT, Kanpur, 2000.

Deb, K. and D. E. Goldberg. An Investigation of Niches and Species Formation in Genetic Function Optimization. In Proc. The Third International Conference on Genetic Algorithms. Ed by J. D. Schaffer, 42. San Mateo, CA: Morgan Kaufmann, 1991.

Dietze, M. and H. Kunhe. Development and Design of Commercial Reactors for Continuous Manufacture of Polyester. *Chemiefasern*, **3**, 19, 1969.

Edgar, T. F. and D. M. Himmelblau. Optimization of Chemical Processes. New York: McGraw Hill, 1988.

Farber, J. N., Steady State Multiobjective Optimization of Continuous Copolymerization Reactors, *Polym. Eng. Sci.*, **26**, 499, 1986.

Flory, P. J. Principles of Polymer Chemistry, Cornell University Press, Ithaca, NY, 1953.

Fonseca, C. M. and P. J. Fleming. Genetic Algorithms for Multiobjective Optimization: Formulation, Discussion and Generalization. In. Proc. The Fifth International Conference on Genetic Algorithms. Ed by S. Forrest. 416, San Mateo, CA: Morgan Kaufmann, 1993.

Fonseca, C. M. and P. J. Fleming. Multiobjective Optimization and Multiple Constraint Handling with Evolutionary Algorithms – Part – I: A Unified Formulation. IEEE Trans. Syst. Man Cy., A, **28**, 26, 1998a.

Fonseca, C. M. and P. J. Fleming. Multiobjective Optimization and Multiple Constraint Handling with Evolutionary Algorithms – Part – II: Application Example. IEEE Trans. Syst. Man Cy., A, **28**, 38-47, 1998b.

Garg, S., and S. K. Gupta. Multiobjective Optimization of a Free Radical Bulk Polymerization Reactor Using Genetic Algorithm, *Macromol. Theor. Simul.*, **8,** 46, 1999.

Garg, S., S. K. Gupta, and D. N. Saraf. On-Line Optimization of Free Radical Bulk Polymerization Reactors in the Presence of Equipment Failure, *J. Appl. Polym. Sci.*, **71**, 2101, 1999.

Ghosh, A. K., A. Kumar and S.K. Gupta. Comments on 'Simplified Analysis of the Performance of Wiped Film Polycondensation Reactors'. *Ind. Eng. Chem. Fundam.*, **22**, 268, 1983.

Goldberg, D. E., Genetic Algorithms in Search, Optimization and Machine Learning, Addision-Wesley, Reading, MA, 1989.

Goldberg, D. E. and J. Richardson. Genetic Algorithms with Sharing for Multimodal Function Optimization. In Proc. The Second International Conference on Genetic Algorithms. Ed by J. J. Grefenstette. 41. Princeton, NJ: Lawrence Erlbaum. 1987.

Gupta, S. K.. Simulation and Optimization of PET Reactors. *Proc. Indian Acad. Sci.,* **92**, 673, 1983.

Gupta, S. K., A. Ghosh, S. K. Gupta and A. Kumar. Analysis of Wiped Film Reactors Using the Orthogonal Collocation Technique, *J. Appl. Polym. Sci.,* **29**, 3217, 1984.

Gupta, S. K. and A. Kumar, Reaction Engineering of Step-Growth Polymerization, Plenum, New York, 1987.

Gupta, S. K.. Numerical Methods for Engineers, New Age International, New Delhi, 1995.

Goicoechea, A., D. R. Hansen, and L. Duckstein. Multiobjective Decision Analysis with Engineering and Business Applications. New York: Wiley, 1982.

Haimes, Y. Y. Hierarchical Analyses of Water Resources Systems: Modeling and Optimization of Large-Scale Systems. New York: McGraw-Hill International Book Co. 1977.

Hipp, A. K. and W. H. Ray. A Dynamic Model for Condensation Polymerization in Tubular Reactors. *Chem. Eng. Sci.,* **51**, 281, 1996.

Holland, J. H. Adaptation in Natural and Artificial Systems. Ann Arbor, Michigan: MIT Press, 1975.

Horn. J., N. Nafpliotis And D. E. Goldberg. A Niched Pareto Genetic Algorithm for Multiobjective Optimization. In Proc. Of The First IEEE Conference on Evolutionary Computation, 82, 1994.

Hovenkamp, S. G. and J. P. Munting. Formation of Diethylene Glycol as a Side Reaction During Production of Polyethylene Terephthalate. *J. Polym. Sci., A-1*, **8**, 679, 1970.

Hovenkamp, S. G.. Kinetic Aspects Catalyzed Reactions in the Formation of Polyethylene Terephthalate. *J.Polym. Sci., A-1*, **9**, 3617, 1971.

Jacobsen, L. L. and W. H. Ray. Unified Modeling Polycondensation Processes. *J. Macromol. Sci.,Rev. Macromol. Chem. Phys.,* **C32**, 911, 1992a.

Jacobsen, L. L. and W. H. Ray. Analysis and Design of Melt and Solution Polycondensation Process. *AIChEJ,* **38**, 911, 1992b.

James, D. E., and L. G. Packer, Effect of Reaction Time on Poly(ethylene terephthalate) Properties, *Ind. Eng. Chem. Res.,* **34**, 4049, 1995.

Kumar, A., S. K. Gupta and N. Somu. MWD of Polyethyelene Terephthalate in HCSTRs. *Polym. Eng. Sci.,* **22**, 314, 1982a.

Kumar, A., S. K. Gupta, B. Gupta and D. Kunzru. Modeling of a Reversible Batch PET Reactor. *J. Appl. Polym. Sci.,* **27**, 4421, 1982b.

Kumar, A., S. K. Gupta, N. Somu and M.V.S. Rao. Simulation of Cyclics and Degradation Product Formation in PET Reactors. *Polymer,* **24**, 449, 1983.

Kumar, A., S. K. Gupta, S. Madan, N. G. Shah and S. K. Gupta. Solution of Final Stages of PET Reactors using Orthogonal Collocation Technique. *Polym. Eng. Sci.,* **24**, 194, 1984a.

Kumar, A., S. N. Sharma and S. K. Gupta. Optimization of Polycondensation Stage of PET Reactors. *J. Appl. Polym. Sci.,* **29**, 1045, 1984b.

Kumar, A., S. N. Sharma and S. K. Gupta. Optimization of the Polycondensation Step of PET Formation with Continuous Removal of Condensation Products. *Polym. Eng. Sci.,* **24**, 205, 1984c.

Kumar, A., V. K. Sukthankar, C.P. Vaz and S. K. Gupta. Optimization of the Transesterification of PET Reactors. *Polym. Eng. Sci.,* **24**, 185, 1984d.

Lapidus, L. and R. Luus. Optimal Control of Engineering Proceses. Waltham :Blaisdell. 1967

Lapidus, L. and B. Lecorre and K. Y. Choi. Two-Phase Model for Continuous Final Stage Melt Polycondensation of Poly (Ethylene Terephthalate). 1. Steady-State Analysis. Ind. Eng. Chem. Res., **30**, 2, 1991.

Laubriet, C., B. LeCorre and K.Y. Choi. Two-Phase Model for continuous Final Stage Melt Polycondensation of Poly (ethylene Terephthalate). 1. Steady-State Analysis. *Ind.Eng.Chem.Res.*, **30**, 2, 1991.

Lei, G. D. and K. Y. Choi. A Melt Prepolymerization of Poly(ethylene Terephthalate) in Semibatch Stirred Reactors. *J. Appl. Polym. Sci.*,**41**, 2987, 1990.

Mitra, K., K. Deb and S. K. Gupta. Multiobjective Dynamic Optimization of an Industrial Nylon 6 Semibatch Reactor Using Genetic Algorithm. *J. Appl. Polym. Sci.,* **69**, 1998.

Pareto, V. Cours D'economie Politique, Lausanne, Switzerland, 1896.

Rajesh, J. K., S. K. Gupta, G. P. Rangaiah and A. K. Ray. Multiobjective Optimization of Steam Reformer Performance Using Genetic Algorithm, *Ind. Eng. Chem. Res.*, **39**, 706, 2000.

Ravindranath, K., and R. A. Mashelkar. Modeling of Polyethylene Terephthalate Reactors. 4. A continuous Esterification Process. *Polym. Eng. Sci.,* **22**, 610, 1982a.

Ravindranath, K., and R. A. Mashelkar. Modeling of Polyethylene Terephthalate Reactors. 5. A continuous Prepolymerization Process. *Polym. Eng. Sci.,* **22**, 619, 1982b.

Ravindranath, K., and R. A. Mashelkar. Modeling of Polyethylene Terephthalate Reactors. 6. A continuous Process for Final Stages of Polycondensation. *Polym. Eng. Sci.*, **22**, 628, 1982c.

Ravindranath, K., and R. A. Mashelkar . Finishing Stages of PET synthesis: A comprehensive Model. *AIChE J.*, **30**, 415, 1984.

Ravindranath, K., and R. A. Mashelkar. Polyethylene Terephthalate – I. Chemistry, Thermodynamics and Transport Properties. *Chem Eng.Sci.,* **41**, 2197, 1986a.

Ravindranath, K., and R. A Mashelkar. Polyethylene Terephthalate – II. Engineering Analysis. *Chem Eng.Sci.,* **41**, 2969, 1986b.

Ray, W. H. and J. Szekely. Process Optimization, with Application in Metallurgy and Chemical Engineering. New York : Wiley, 1973.

Saint Martin, H. S. and K.Y. Choi. Two-Phase Model for Continuous Final Stage Melt Polycondensation of Poly (ethylene Terephthalate). 2. Analysis of Dynamic Behavior. *Ind.Eng.Chem.Res.,* **30**, 1712, 1991.

Schaffer, J. D. Some experiments in Machine Learning Using Vector Evaluated Genetic Algorithms. Ph. D. Thesis, vanderbilt University, Nashville, TN, USA, 1984.

Secor, R. M.. The Kinetics of Condensation Polymerization. *AIChE J.*, **15**, 861, 1969.

Srinivas, N. and K. Deb. Multiobjective Function Optimization using Nondominated Sorting Genetic Algorithms. Evolutionary Computation, **2**, 221, 1995.

Steppan, D.D., M.F. Doherty and M.F. Malone. Wiped Film Reactor Model for Nylon 6,6 Polymerization. *Ind. Eng. Chem. Res.*, **29**, 2012. 1990.

Wajge. R.M. and S. K. Gupta. Multiobjective Dynamic Optimization of a Nonvaporizing Nylon 6 Batch Reactor. *Polym. Eng. Sci.,* **34**, 1161, 1994.

Zabisky, R. C. M., W. M. Chan, P. E. Gloor and A. E. Hamielec. A Kinetic-Model for Olefin Polymerization in High-Pressure Tubular Reactors - A Review and Update. *Polymer*, **33**, 2243, 1992.